

A Novel Fatty Acyl-CoA Synthetase Is Required for Pollen Development and Sporopollenin Biosynthesis in *Arabidopsis*

Clarice de Azevedo Souza,^{a,1} Sung Soo Kim,^a Stefanie Koch,^b Lucie Kienow,^b Katja Schneider,^{b,2} Sarah M. McKim,^a George W. Haughn,^a Erich Kombrink,^b and Carl J. Douglas^{a,3}

^aDepartment of Botany, University of British Columbia, Vancouver, BC V6T 1Z4, Canada

^bMax Planck Institute for Plant Breeding Research, Department of Plant–Microbe Interactions, 50829 Köln, Germany

Acyl-CoA Synthetase (ACOS) genes are related to 4-coumarate:CoA ligase (4CL) but have distinct functions. The *Arabidopsis thaliana* ACOS5 protein is in clade A of *Arabidopsis* ACOS proteins, the clade most closely related to 4CL proteins. This clade contains putative nonperoxisomal ACOS enzymes conserved in several angiosperm lineages and in the moss *Physcomitrella patens*. Although its function is unknown, ACOS5 is preferentially expressed in the flowers of all angiosperms examined. Here, we show that an *acos5* mutant produced no pollen in mature anthers and no seeds by self-fertilization and was severely compromised in pollen wall formation apparently lacking sporopollenin or exine. The phenotype was first evident at stage 8 of anther development and correlated with maximum ACOS5 mRNA accumulation in tapetal cells at stages 7 to 8. Green fluorescent protein–ACOS5 fusions showed that ACOS5 is located in the cytoplasm. Recombinant ACOS5 enzyme was active against oleic acid, allowing kinetic constants for ACOS5 substrates to be established. Substrate competition assays indicated broad *in vitro* preference of the enzyme for medium-chain fatty acids. We propose that ACOS5 encodes an enzyme that participates in a conserved and ancient biochemical pathway required for sporopollenin monomer biosynthesis that may also include the *Arabidopsis* CYP703A2 and MS2 enzymes.

INTRODUCTION

Anther development and the development of haploid microspores and mature male gametophytes (pollen grains) is a complex process central to the angiosperm life cycle. Stages of anther development and microsporogenesis are precisely timed and tightly controlled and are characterized by specific events ranging from initial cell differentiation from the floral meristem to pollen formation, maturation, and release during anther dehiscence. In tobacco (*Nicotiana tabacum*) and *Arabidopsis thaliana*, anther development has been divided into stages based on anatomical, morphological, cellular, and molecular events (Goldberg et al., 1993; Sanders et al., 1999; Scott et al., 2004; Ma, 2005). Molecular genetic studies, particularly in *Arabidopsis*, have shed light on events in anther development and microsporogenesis (Ma, 2005). However, many biochemical and cellular processes specific to anther development and their regulation are still uncharacterized.

One event of fundamental importance during pollen maturation is the deposition of the pollen wall, necessary for pollen protection, dispersal, and pollen-stigma recognition (Piffanelli et al., 1998; Scott et al., 2004). The pollen wall is among the most complex plant extracellular matrices and consists of multiple layers. A microspore-derived cellulosic primexine is synthesized by the developing haploid microspores at the tetrad stage (Blackmore et al., 2007). A thick exine, whose components are synthesized by the sporophyte, is deposited on the outer surface of the primexine largely after release of free microspores, and a pectocellulosic intine is produced by developing microspores and male gametophytes and deposited internally to the exine (Blackmore et al., 2007). Since *Arabidopsis* plants with mutations in three cellulose synthase *CESA* genes involved in primary wall formation are male sterile and exhibit aberrant pollen wall formation, cellulose deposition by the haploid microspores is known to be important for pollen wall development and pollen fertility (Persson et al., 2007).

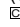
Constituents of the maternally derived exine are produced in the tapetal cell layer that surrounds the inner surface of the anther locules (Piffanelli et al., 1998). After secretion into the locules, exine precursors are deposited and polymerized on the surface of the primexine, by unknown mechanisms, to form the thick exine wall that is extremely resistant to degradation (Piffanelli et al., 1998; Scott et al., 2004; Ma, 2005; Vizcay-Barrena and Wilson, 2006; Zhang et al., 2006). A primary constituent of the exine is sporopollenin, an enigmatic polymer of aliphatic and aromatic constituents coupled via extensive ester and ether linkages that is extremely resistant to degradation (Scott et al., 2004; Ma, 2005). The exine not only contributes to the remarkable resistance of the pollen wall to abiotic and biotic stresses, such as

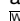
¹ Current address: Department of Microbiology and Immunology, University of Miami, Leonard Miller School of Medicine, Miami, FL 33136.

² Current address: Gene Discovery Research Group, Riken Yokohama Institute, Plant Science Center, Yokohama 230-0045, Japan.

³ Address correspondence to cdouglas@interchange.ubc.ca.

The author responsible for distribution of materials integral to the findings presented in this article in accordance with the policy described in the Instructions for Authors (www.plantcell.org) is: Carl J. Douglas (cdouglas@interchange.ubc.ca).

 Some figures in this article are displayed in color online but in black and white in the print edition.

 Online version contains Web-only data.

www.plantcell.org/cgi/doi/10.1105/tpc.108.062513

dehydration, UV irradiation, and pathogen attack, but also facilitates pollen–stigma interactions (Eclund et al., 2004).

In addition to their role in sporopollenin monomer biosynthesis, tapetal cells are active in the biosynthesis of steryl esters, long-chain alkanes, and flavonoids (Hsieh and Huang, 2007). After synthesis and deposition of the pollen wall, the tapetal cells are degraded via programmed cell death, resulting in the release of these constituents into the locule where they form a complex lipid coat on the outer surface of pollen grains (Piffanelli et al., 1998; Hsieh and Huang, 2005), the ultimate step in formation of the pollen grain extracellular matrix.

While recent progress has been made in understanding the structure and biosynthesis of two other major aliphatic-based polyester extracellular matrices that share many similarities to sporopollenin (i.e., cutin and suberin) (reviewed in Franke and Schreiber, 2007; Pollard et al., 2008), the structure and monomeric composition of the exine and the sporopollenin polymer remain largely unknown due to the small amounts of material made during microspore and pollen grain development, the recalcitrance of exine to chemical degradation, and the limited number of techniques available for exine chemical analysis (Dominguez et al., 1999; Bubert et al., 2002; Ahlers et al., 2003; Blokker et al., 2005). Available data from several plants indicate that the major monomeric components of the sporopollenin polymer are polyhydroxylated, unbranched long-chain, and/or very-long-chain fatty acids, as well as oxygenated aromatic compounds, likely derived from phenylpropanoid acids, such as *p*-coumaric, caffeic, and/or ferulic acids (Guilford et al., 1988; Ahlers et al., 1999; Dominguez et al., 1999; Ahlers et al., 2000; Blackmore et al., 2007). While the nature of the sporopollenin structure and the monomer building blocks has not been clearly defined, data from chemical degradation of isolated sporopollenin suggest that there are a limited number of monomeric constituents (Bubert et al., 2002). It has also been recognized that there are chemical similarities between the walls of spores in the descendants of early land plants, such as bryophytes and lycopods, and those of pollen grains (Morant et al., 2007). Thus, a key innovation in the colonization of the terrestrial environment by the first land plants 600 to 450 million years ago may have been the acquisition of the ability to generate the sporopollenin polymer to protect haploid spores (Bowman et al., 2007; Morant et al., 2007), and sporopollenin may have been one of the first plant polyester-based extracellular matrices to have evolved (Morant et al., 2007).

Numerous male sterile or partially sterile mutants that have been isolated and characterized in *Arabidopsis* define some of the key processes in anther and male gametophyte development (Taylor et al., 1998; Sanders et al., 1999; Ma, 2005). Male sterile mutants displaying apparently normal microspore and tapetum development, but with defects in pollen wall formation and pollen maturation, have started to shed light on the cell biology and biochemistry of pollen wall, exine, and sporopollenin development and biosynthesis. For example, the *male sterile2* (*ms2*) mutant, defective in sporopollenin deposition, develops microspores that collapse shortly after release from tetrads, showing no signs of pollen wall formation. The MS2 protein accumulates specifically in the tapetum and was suggested to be a long-chain fatty acid reductase that is involved in the biosynthesis of a long-

chain aliphatic component of the sporopollenin polymer (Aarts et al., 1997). In the *defective in exine formation1* (*dex1*) mutant, abnormal microspores develop after release from tetrads and eventually collapse, as in the *ms2* mutant, because the sporopollenin that is produced does not anchor to the developing pollen grains (Paxson-Sowders et al., 2001). DEX1 is a novel protein of unknown function thought to be localized to the plasmalemma. Other genes associated with exine production and male fertility include *YORE-YORE/WAX2/FACELESSPOLLEN1*, encoding an enzyme apparently involved in wax biosynthesis (Ariizumi et al., 2003; Chen et al., 2003; Kurata et al., 2003) and the rice (*Oryza sativa*) *Wax-deficient anther1* gene, a homolog of the *Arabidopsis* *ECERIFERUM1* gene that encodes a putative membrane protein apparently required for very-long-chain fatty acid metabolism (Jung et al., 2006).

Recently, the *Arabidopsis* cytochrome P450 enzyme CYP703A2 has been shown to be required for the biosynthesis of sporopollenin precursors. CYP703A2 knockout mutants (*dex2*) are partially male sterile, with poorly developed exine, and apparently lack sporopollenin (Morant et al., 2007). CYP703A2 appears to function in vitro as a fatty acid in-chain hydroxylase that preferentially generates 7-hydroxy lauric acid, which is proposed to be a sporopollenin precursor (Morant et al., 2007). The conservation of the CYP703 clade in bryophytes and other land plant lineages suggests that the enzyme participates in an ancient, conserved biochemical pathway for sporopollenin biosynthesis (Morant et al., 2007).

Novel classes of *Arabidopsis* genes encoding enzymes related to, yet functionally distinct from, phenylpropanoid genes have been defined (phenylpropanoid-like genes; Costa et al., 2003; Raes et al., 2003; Ehling et al., 2005). Many such genes are conserved in the fully sequenced genomes of poplar (*Populus trichocarpa*) and rice (*Oryza sativa*) (Tuskan et al., 2006; Hamberger et al., 2007; de Azevedo Souza et al., 2008). An example of such a supergene family is the group of genes encoding adenylate-forming enzymes related to the phenylpropanoid enzyme 4-coumarate:CoA ligase (4CL) (Cukovic et al., 2001; Costa et al., 2003, 2005; Schneider et al., 2003, 2005; Shockey et al., 2003; Ehling et al., 2005; de Azevedo Souza et al., 2008). Recent biochemical characterizations of enzymes encoded by this family of 4CL-like genes show that they generally do not convert substrates accepted by true 4CL enzymes to the corresponding CoA esters (Costa et al., 2005; Kienow et al., 2008). Instead, many accept fatty acyl substrates, such as 12-oxo-phytodienoic acid (OPDA) and OPDA derivatives (jasmonic acid precursors; Koo et al., 2006; Kienow et al., 2008), and medium- to long-chain fatty acids (Kienow et al., 2008). Based on such activities, we have designated those 4CL-like genes with unknown in vivo substrates as *Acyl-CoA Synthetase* (ACOS; formerly referred to as the ACS class of genes; de Azevedo Souza et al., 2008). This class of genes is distinct from those encoding long-chain acyl-CoA synthetases (LACS; Shockey et al., 2002), such as the *Arabidopsis* *LACS2* gene, which is required for cutin biosynthesis (Schnurr et al., 2004), or the *LACS6* and *LACS7* genes, involved in storage lipid degradation (Fulda et al., 2004). A recent genome-wide phylogenetic analysis of ACOS genes shows that variable numbers of ACOS homologs are present in the poplar, rice, and *Physcomitrella patens*

genomes but that they are absent from *Chlamydomonas reinhardtii* (de Azevedo Souza et al., 2008).

Most ACOS genes identified in *Arabidopsis* and other species are predicted to localize to peroxisomes, based on the presence of C-terminal peroxisomal targeting sequences (Costa et al., 2005; Schneider et al., 2005; de Azevedo Souza et al., 2008), and this is consistent with their having roles in fatty acid and jasmonate metabolism, which occur in this cellular compartment (Schneider et al., 2005; Koo et al., 2006; Kienow et al., 2008). One ACOS clade identified in this analysis is unique in that it contains single-copy genes from *Arabidopsis*, poplar, and rice, which all encode enzymes without predicted peroxisomal targeting sequences (de Azevedo Souza et al., 2008). The *Arabidopsis* gene in this clade, ACOS5, is preferentially expressed in flowers (Douglas and Ehling, 2005; de Azevedo Souza et al., 2008), whereas expression of the poplar ortholog is mainly in male flowers (de Azevedo Souza et al., 2008). Thus, a function for ACOS5 in anther development has been proposed (de Azevedo Souza et al., 2008).

In this study, we characterized a loss-of-function allele of the *Arabidopsis* ACOS5 gene, *acos5-1*, and showed that *acos5-1* homozygotes are completely male sterile, with no pollen observed in mature anthers and no seeds produced by self-fertilization. Further analyses demonstrated that ACOS5 is a medium- to long-chain fatty acyl-CoA synthetase that is required in tapetal cells for sporopollenin monomer biosynthesis. Light and transmission electron microscopy studies indicated that the defect in pollen development in the *acos5* mutant coincides with exine deposition at the unicellular stage, which is completely lacking in the mutant. Our data indicate that ACOS5 encodes an acyl-CoA synthetase protein that participates in an ancient biochemical pathway required for sporopollenin monomer biosynthesis, providing novel insight into the reactions underlying the biosynthesis of this important polymer.

RESULTS

***Arabidopsis* ACOS5 Is a Member of an Ancient and Conserved Clade of Nonperoxisomal 4CL-Like Genes**

Previous results showed that the *Arabidopsis* 4CL-like gene ACOS5 is a single-copy gene with homologs in the genomes of

representative fully sequenced land plants (de Azevedo Souza et al., 2008). To further clarify the relationship between ACOS5, its homologs, and true 4CL genes in plants, we used the corresponding protein sequences from *Arabidopsis*, poplar, rice, the moss *Physcomitrella*, and tobacco (*Nicotiana sylvestris*) (as listed in Table 1; see Supplemental Table 1 online) to construct an unrooted maximum likelihood phylogenetic tree (Figure 1; see Supplemental Data Set 1 online). In this phylogenetic reconstruction, we included homologs from each of the plants examined and found that clade A ACOS genes form a distinct phylogenetic sister group to 4CLs. In contrast with bona fide 4CL genes, which have undergone complex patterns of gene family expansion in different lineages (Figure 1), clade A ACOS proteins are encoded by single-copy genes in each of the four species analyzed for which the complete genome sequences are available. Also, according to this analysis, the *Physcomitrella* clade A ACOS gene (ACOS6) and the four *Physcomitrella* sequences that encode 4CL proteins (Silber et al., 2008) are basal to the angiosperm clade A ACOS genes and to angiosperm 4CL genes, respectively (Figure 1). This suggests that both 4CL and clade A ACOS genes arose early in land plant evolution and were present in the most recent common ancestor of angiosperms and *Physcomitrella*. Consistent with this, no clade A ACOS genes were found in the *C. reinhardtii* genome (Table 1).

Unlike most other 4CL-like ACOS proteins, *Arabidopsis* ACOS5 and its homologs in other species do not contain recognizable peroxisomal targeting sequences of type 1 at their C termini (de Azevedo Souza et al., 2008). To empirically test the subcellular localization of ACOS5, we generated a yellow fluorescent protein (YFP)-tagged variant that was placed under the control of the cauliflower mosaic virus 35S promoter (p35S:YFP-ACOS5) and transiently expressed this construct together with a reporter construct of a peroxisomal marker protein (p35S:RFP-SRL reporter) (Schneider et al., 2005). Red fluorescent protein (RFP) and YFP localization in single *Arabidopsis* epidermal cells was assayed by confocal laser scanning microscopy using appropriate filter sets for simultaneous and selective recording of RFP and YFP (Figure 2). While RFP-SRL-expressing cells displayed a punctate pattern typical of peroxisomal localization, YFP-ACOS5 localization did not coincide with this pattern; instead, YFP fluorescence was primarily restricted to the cytoplasm (Figure 2). This suggests that the ACOS5 enzyme is localized to the cytoplasm.

Table 1. Putative ACOS5 Orthologs and Expression in Other Species

Species	Gene name	Accession or Gene Model	Expression
<i>Arabidopsis</i>	ACOS5	At1g62940	Tapetum ^a
<i>P. trichocarpa</i>	ACOS13	eugene3.00010460	Male flower ^b
<i>O. sativa</i>	ACOS12	Os04g24530	Immature panicle ^c
<i>N. sylvestris</i>	CL-1k	AY163489	Tapetum ^d
<i>P. patens</i>	ACOS6	fgenes1_pg.scaffold_96000119	NA ^e
<i>C. reinhardtii</i>	No hit		

^aThis study.

^bFrom de Azevedo Souza et al. (2008).

^cFrom <http://mpss.udel.edu/rice/>.

^dFrom Varbanova et al. (2003).

^eNA, no information available.

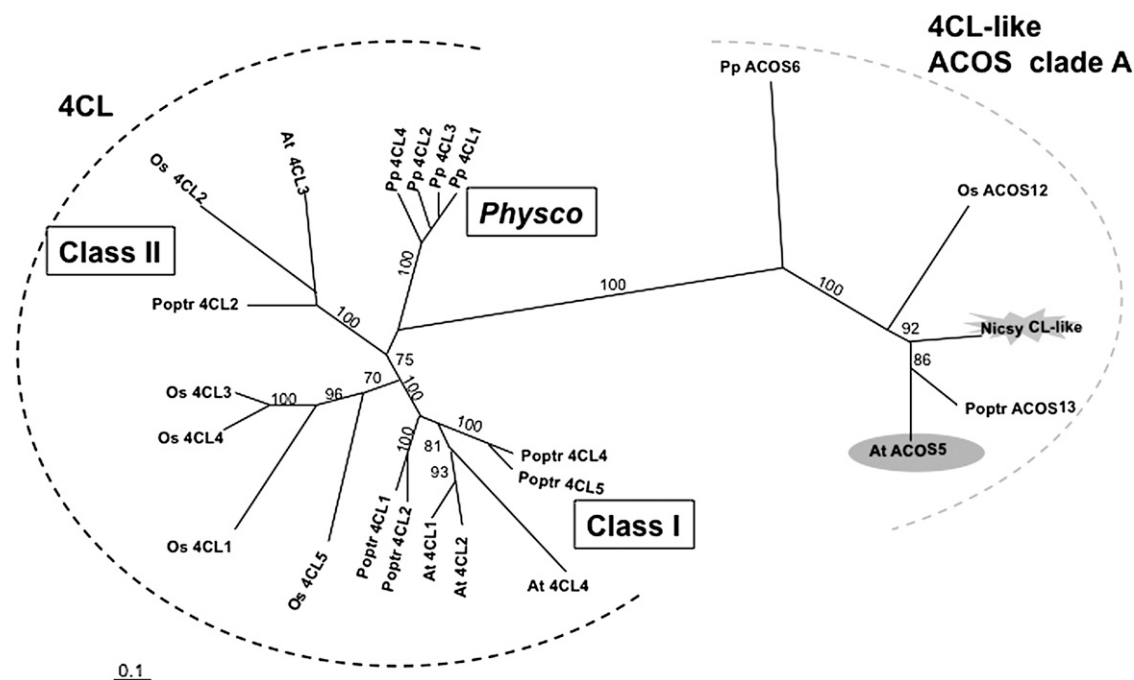


Figure 1. Phylogenetic Analysis of Selected 4CL and 4CL-Like ACOS Protein Sequences.

Sequences from *Arabidopsis*, poplar, rice, *Physcomitrella*, and *Nicotiana* were aligned and used to construct an unrooted maximum likelihood tree using PhyML 2.4.4. Bootstrap values (1000 replicates) above 70% are shown on branches. The protein encoded by an *N. sylvestris* gene expressed in tapetal cells during anther development is indicated by a flash. Class I and II 4CL subclasses as defined by Ehling et al. (1999) and a *Physcomitrella* 4CL subclass are indicated by boxed text. Genes used in this analysis are given in Supplemental Table 1 online, and the sequences used to generate this phylogeny are provided in Supplemental Data Set 1 online. Bar = 0.1 amino acid substitutions.

Identification of an ACOS5 Loss-of-Function Allele

Previous experiments showed that *Arabidopsis* ACOS5 has a flower-preferred expression pattern, that the poplar homolog ACOS13 is expressed in male but not in female flowers (de Azevedo Souza et al., 2008), and that the *N. sylvestris* homolog *CL-lk* is expressed specifically in the tapetum of developing anthers (Varbanova et al., 2003). To explore the organ- and cell type-specific expression pattern of ACOS5, promoter sequences of variable length (1030, 1416, and 1620 bp) were fused to the β -glucuronidase (*GUS*) reporter gene and integrated into the *Arabidopsis* genome. Several independent transgenic lines homozygous for a single copy of the *ProACOS5:GUS* gene fusion were analyzed for *GUS* activity. All lines yielded identical results, and representative data are shown in Figure 3. No *GUS* expression was observed in vegetative organs of seedlings and plants (i.e., cotyledons, leaves, roots, and stems; Figures 3A and 3B). However, *GUS* expression was first evident in young flower buds at developmental stages 7 to 9 according to Sanders et al. (1999) where it was restricted specifically to the developing anthers (Figures 3D to 3F). Beyond stage 9, *GUS* expression rapidly declined, with no *GUS* staining being detectable at anther maturity (Figure 3C).

We obtained an ACOS5 transposon insertion line (SM_3.37225) from the Nottingham Arabidopsis Stock Centre (NASC). Within the segregating population, plants homozygous for the ACOS5

insertion allele (*acos5-1*) were identified by PCR genotyping, and the location of the transposon insertion in the second exon of ACOS5 was verified (Figure 4A). We assayed ACOS5 expression by RT-PCR in both wild-type and mutant flowers. Using primers flanking the insertion site, no ACOS5 mRNA could be detected in the mutant, indicating that functional ACOS5 mRNA does not accumulate in the mutant and that *acos5-1* is likely to be a null allele of ACOS5 (Figure 4A).

Initial phenotypic analysis of the homozygous *acos5-1* plants suggested that the plants were self-sterile, since siliques failed to mature and produce seeds. Careful examination of the mutant flowers revealed anthers that were apparently devoid of pollen grains (Figure 5A). At a time when flowers of wild-type plants grown in parallel had self-pollinated and produced siliques with developing seeds, development of *acos5* mutant flowers culminated in undeveloped siliques and complete absence of seed production (Figure 5A). There were no other obvious morphological differences between the *acos5* mutant and wild-type plants grown to maturity (Figure 5A), except that *acos5* mutant plants flowered for a longer time (Figure 5A), consistent with observations of other male sterile mutants (Aarts et al., 1997).

Secondary wall formation and lignin deposition in anther endothecium cells is required for anther dehiscence and pollen release (Dawson et al., 1999; Yang et al., 2007). Given the close relationship between ACOS5 and 4CL genes, we considered

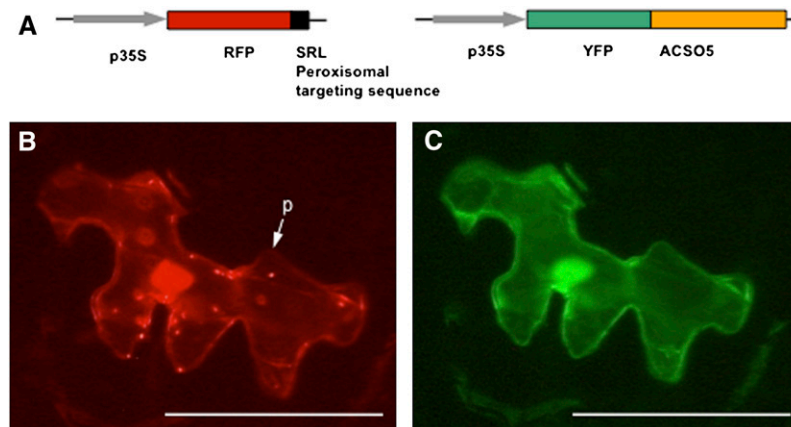


Figure 2. Subcellular Localization of ACOS5 in *Arabidopsis* Leaf Epidermal Cells.

(A) Structural features of the reporter constructs *p35S:RFP-SRL*, with the synthetic C terminus –SRL serving as peroxisomal marker, and *p35S:YFP-ACOS5* both under the control of the cauliflower mosaic virus 35S promoter (*p35S*).

(B) and **(C)** Both expression plasmids were cotransformed into *Arabidopsis* leaves by particle bombardment. Single epidermal cells were inspected by confocal laser scanning microscopy using appropriate filter sets for simultaneous and selective recording of RFP **(B)** and YFP **(C)** fluorescence. Optical sections were acquired for the reconstruction of three-dimensional images of the cellular labeling patterns and indicate that the YFP signal is primarily restricted to the cytoplasm and does not coincide with the punctate RFP fluorescence pattern of the peroxisomal marker (p). Bar = 25 μ m.

the possibility that the enzyme encoded by *ACOS5* is required for lignin biosynthesis in the endothecium and that lack of lignification and anther dehiscence resulted in the loss of pollen release. To test this, we treated anthers in developing wild-type and *acos5-1* mutant flowers with phloroglucinol, which stains lignin and other wall-bound phenolics. However, anthers from both wild-type and *acos5-1* mutant plants stained equally well, suggesting that there is no defect in lignin deposition in the mutant and that *ACOS5* activity is not required for lignin biosynthesis in the anther (Figure 5B).

To investigate the basis for the failure of self-pollination in *acos5* mutant plants, we used scanning electron microscopy to view anther development at higher resolution in wild-type and mutant flowers. *acos5* mutant anthers underwent apparently normal development and dehiscence, but no pollen grains could be observed either in dehiscing anthers or attached to stigmata; by contrast, abundant pollen was observed in dehiscing wild-type anthers examined in parallel (see Supplemental Figure 1 online). The absence of pollen in *acos5* mutant flowers, as observed by light or scanning electron microscopy, indicates that *ACOS5* function is absolutely required for pollen maturation. When *acos5* mutant plants were used as pollen recipients in crosses with pollen from wild-type plants, siliques developed normally and produced F1 seeds that germinated normally with no apparent loss in fecundity relative to self-pollinated wild-type plants.

Since only one insertional mutant line was available for *ACOS5*, we allowed the F1 heterozygote plants derived from the above cross to self-pollinate to test the resulting F2 population for cosegregation of the male sterile phenotype with *acos5-1*. In this population, the male sterile mutant phenotype was inherited in a Mendelian fashion, with one-quarter of the 184 F2 progeny displaying male sterility ($\chi^2 = 0.437$; $P > 0.4$; $n = 184$), illustrating that the mutant phenotype is caused by a mutation at a single

locus. Next, we determined the genotypes of 183 F2 plants. This analysis showed that the male sterile phenotype cosegregated with *acos5-1* (51/51 *acos5-1* homozygotes were male sterile, whereas all 132 individuals that were either *ACOS5/acos5-1* heterozygotes or *ACOS5* homozygotes were fertile). This strongly suggests that the male sterile phenotype and the complete block of pollen formation were caused by loss of function of the *ACOS5* gene.

To test for the ability of the *ACOS5* gene to complement the male sterile phenotype in the *acos5-1* background, we introduced an ~ 4.4 -kb DNA region from an *Arabidopsis* wild-type (Columbia-0 [Col-0]) plant, containing 1.9 kb of the promoter sequence and the complete transcribed region of *ACOS5* (Figure 4B), into *ACOS5/acos5-1* heterozygote plants by *Agrobacterium tumefaciens*-mediated transformation. Four T1 lines harboring the *ACOS5* transgene were subjected to PCR-aided genotyping, and one was established as being *ACOS5/ACOS5*, one as being *ACOS5/acos5-1*, and two as being *acos5-1/acos5-1*. All plants were fully fertile, suggesting that the introduced *ACOS5* transgene had complemented the *acos5-1* mutation in the two homozygous lines. We further determined the genotypes and phenotypes of 18 T2 progeny from each T1 line that had inherited the *ACOS5* transgene (i.e., that was either homozygous or hemizygous for the *ACOS5* transgene, based on hygromycin resistance specified by the T-DNA insertion). For each T1 line, including the two that were homozygous for the *acos5-1* allele and gave rise only to *acos5-1/acos5-1* T2 progeny, all 18 T2 plants were fully fertile, confirming the ability of *ACOS5* to complement the male sterile mutant phenotype.

Anther and Microspore Development in the *acos5-1* Mutant

To identify the point at which pollen development was impaired in the *acos5* mutant, we analyzed anther cross sections taken from

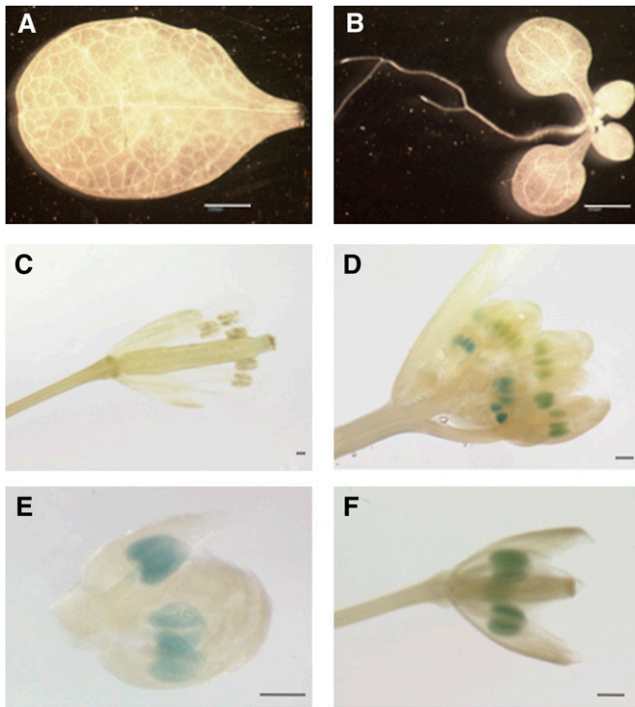


Figure 3. Developmental and Tissue-Specific Expression of the *ACOS5* Gene.

Arabidopsis lines homozygous for a single insertion of the reporter gene, comprising a 1030-bp promoter of the *ACOS5* gene and the GUS reporter, were generated and selected. Reporter activity was revealed by X-gluc staining. Stages are according to Sanders et al. (1999). Bar = 1000 μm in (A), 500 μm in (B), and 150 μm in (C) to (F).

(A) Leaf of three-week-old plant grown on soil.

(B) One-week-old seedling grown on Murashige and Skoog medium.

(C) Fully developed flower at anthesis (stage 12 to 13).

(D) to (F) Young flower buds (stage 7 to 9).

wild-type (Col-0) and *acos5* flowers at different stages of anther development, as defined by Sanders et al. (1999). Representative sections are shown in Figure 6. Early stages of anther development in *acos5* appeared normal. By stage 5, in both mutant and wild-type anthers, four defined locules were established and visible pollen mother cells had appeared. Subsequently, the pollen mother cells underwent meiosis and tetrads were formed, connected by a callose wall (stage 7) in both wild-type and *acos5* plants. In both wild-type and *acos5* mutant anthers, individual microspores could be seen at stage 8, indicating that the callose wall had degenerated, releasing the microspores from the tetrads in a normal manner.

At stage 9, the wild-type pollen grains became vacuolated, and an exine wall started to become visible, as evidenced by toluidine blue staining of the pollen grain walls. However, normal development seemed to be arrested in the *acos5* mutant at this stage. Although the vacuoles were evident in some mutant microspores, microspores appeared malformed and distorted in shape, and exine walls were not as clearly evident as in the wild type (Figure 6). In place of the clearly developing microspores

seen in the locules of wild-type anthers, stage 9 mutant locules were filled with misshapen structures.

During stage 10, wild-type pollen grains continued to enlarge and develop, and the tapetum layer showed initial signs of degeneration. By contrast, in the mutant anthers at an age equivalent to stage 10, we observed degradation of both microspores and the tapetum (Figure 6). Thus, in the *acos5* mutant, no developing pollen grains were observed at this stage, and the tapetum degenerated earlier than in wild-type plants. At stage 11, the tapetal cell layer was greatly degraded in wild-type anthers, and clear darkly staining pollen grains were seen. By contrast, although fully mature anthers appeared otherwise normal in the mutant, the locules were empty, devoid of pollen grains (Figure 6). These data suggest that the *acos5* male sterile phenotype is manifested relatively late in anther and microspore development, at stages 8 and 9 (free microspore stages) when exine formation and sporopollenin deposition occur.

To further pinpoint the stage of anther development defective in the *acos5* mutant, we used transmission electron microscopy to gain higher-resolution images of developing anthers in the *acos5* mutant and compared these to the corresponding images from wild-type plants. Figures 7A to 7D show that, at stage 7, characterized by the presence of tetrads that form after meiosis, wild-type and *acos5* mutant microspores were similar in morphology, with

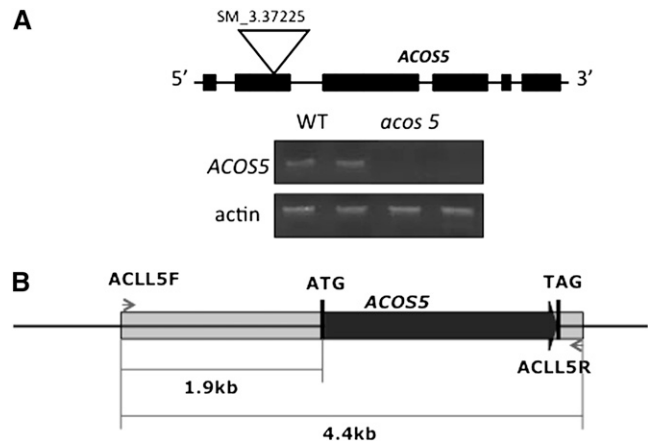


Figure 4. Molecular Characterization of the *acos5-1* Insertion Allele, Effects of the Insertion on Gene Expression, and the Construct Used for Complementation.

(A) Location of the transposon insertion in the second exon of *ACOS5* in the *acos5-1* allele is shown above. Black boxes denote exons, whereas thin horizontal lines denote introns. Below, RT-PCR analysis of *ACOS5* expression in wild-type and *acos5* flowers is shown. Expression was evaluated using intron-spanning primers on either side of the T-DNA insertion as described in Methods. Two biological replicates of the analysis are shown and gave identical results.

(B) Schematic representation of the construct used for the *acos5* complementation test. Shaded boxes show the *ACOS5* transgene, containing 1.9 kb of the promoter sequence, the 3' untranslated region/terminator regions (light gray), and the transcribed region between the start and stop codons (thick black arrow). Primers used to amplify genomic DNA are indicated with arrows above and below the diagram and are shown in Supplemental Table 4 online.

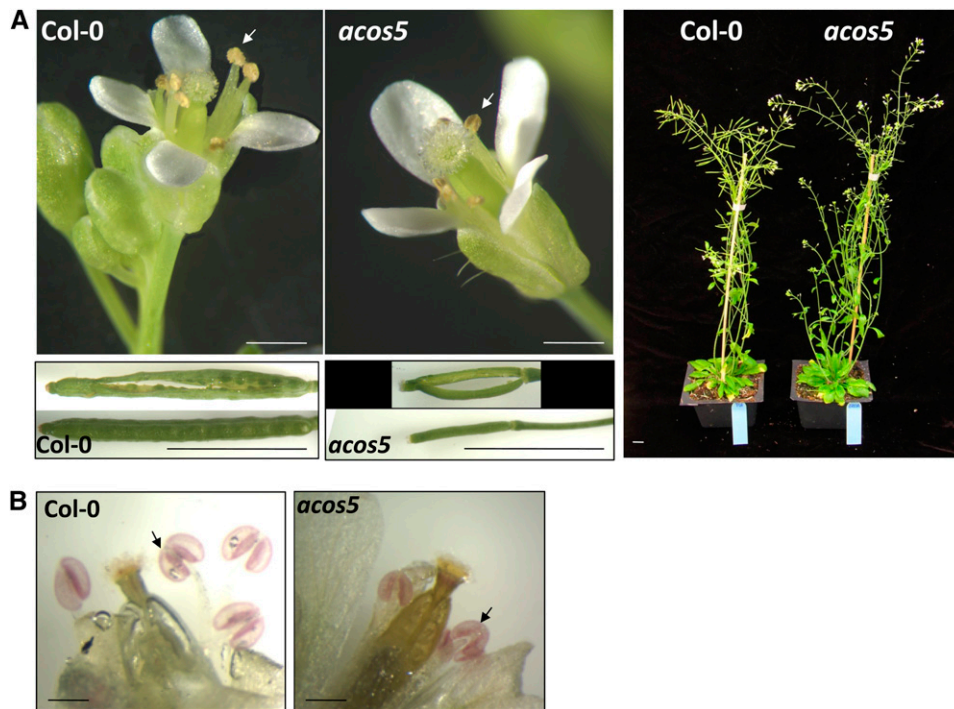


Figure 5. Phenotypic Characterization of *acos5* Plants.

(A) Mature wild-type (Col-0) and *acos5* flowers are shown. Mutant anthers are devoid of pollen, and no pollen grains were attached to the stigma. Siliques devoid of seeds derived from *acos5* homozygotes relative to the wild type (Col-0) are shown below. To the right, the morphology of mature wild-type (Col-0) and *acos5* mutant plants is shown

(B) Lignin and wall-bound phenolic accumulation in wild-type and *acos5* anthers. Mature wild-type (Col-0) and *acos5* flowers were stained with phloroglucinol and showed similar staining patterns in anthers.

characteristic callose walls. At this stage, tapetal cells in the mutant appeared normal. At stage 8, when free microspores had been released from tetrads following callose wall hydrolysis, massive deposition of a thick sporopollenin-containing exine on the nexine layer was evident in the wild-type anthers (Figures 7E and 7F). The exine had started to develop into a thick, reticulated wall characteristic of pollen grains, residual primexine was visible in spaces of exine baculae, which are characteristic of this stage (Goldberg et al., 1993; Sanders et al., 1999; Scott et al., 2004; Ma, 2005), and microspores were nonvacuolated. In comparison with the wild type, free *acos5* mutant microspores at stage 8 had a similar nonvacuolated morphology but contained thinner walls that were devoid of the pronounced reticulate exine wall seen in the wild type (Figures 7G and 7H). In place of a well-defined exine, these microspores contained an amorphous substance adhering to the nexine that could be residual primexine or unpolymerized sporopollenin precursors. Again, tapetal cells at this stage appeared normal.

At stage 9, wild-type pollen grains contained thick, reticulated exine walls and an intine layer. In stage 9 of the *acos5* mutant, many pollen grains were in various stages of lysis and degradation (Figure 7K) and had thin cell walls that were devoid of a characteristic exine layer (Figure 7L) but often retained amorphous wall material outside the intine and apparent nexine. In other cases, relatively intact pollen grains were observed in *acos5*

anthers at stage 9 (Figure 7M), but in many cases, pollen walls were completely devoid of wall material outside the intine (Figure 7N). Again, tapetal cells in the *acos5* mutant anthers appeared normal at this stage (Figures 7K and 7M), suggesting that the defect in *acos5* pollen development is primarily due to the lack of sporopollenin deposition and exine formation, rather than a general defect in tapetal cell development. This analysis pinpoints the defect in microspore development in the *acos5* mutant to the deposition of the sporopollenin-rich exine wall at stages 8 and 9 of anther development, while other aspects of anther development, including tapetal cell development, appear normal.

Localization of ACOS5 Expression in Developing Anthers

To gain insight into the spatio-temporal pattern of ACOS5 expression in anthers, we performed in situ hybridization using an ACOS5-derived probe and developing wild-type flowers. Figure 8A shows that ACOS5 was strongly, specifically, and transiently expressed in the tapetal cell layer of developing anthers. At the beginning of stage 5, locules with microspore mother cells and a distinct tapetum were evident, but no hybridization signal was observed. Toward the end of stage 5, clear but relatively weak hybridization of the probe to the developing tapetum was detected. By stage 7, which is characterized by the presence of tetrads within the locules, maximal hybridization was seen in the

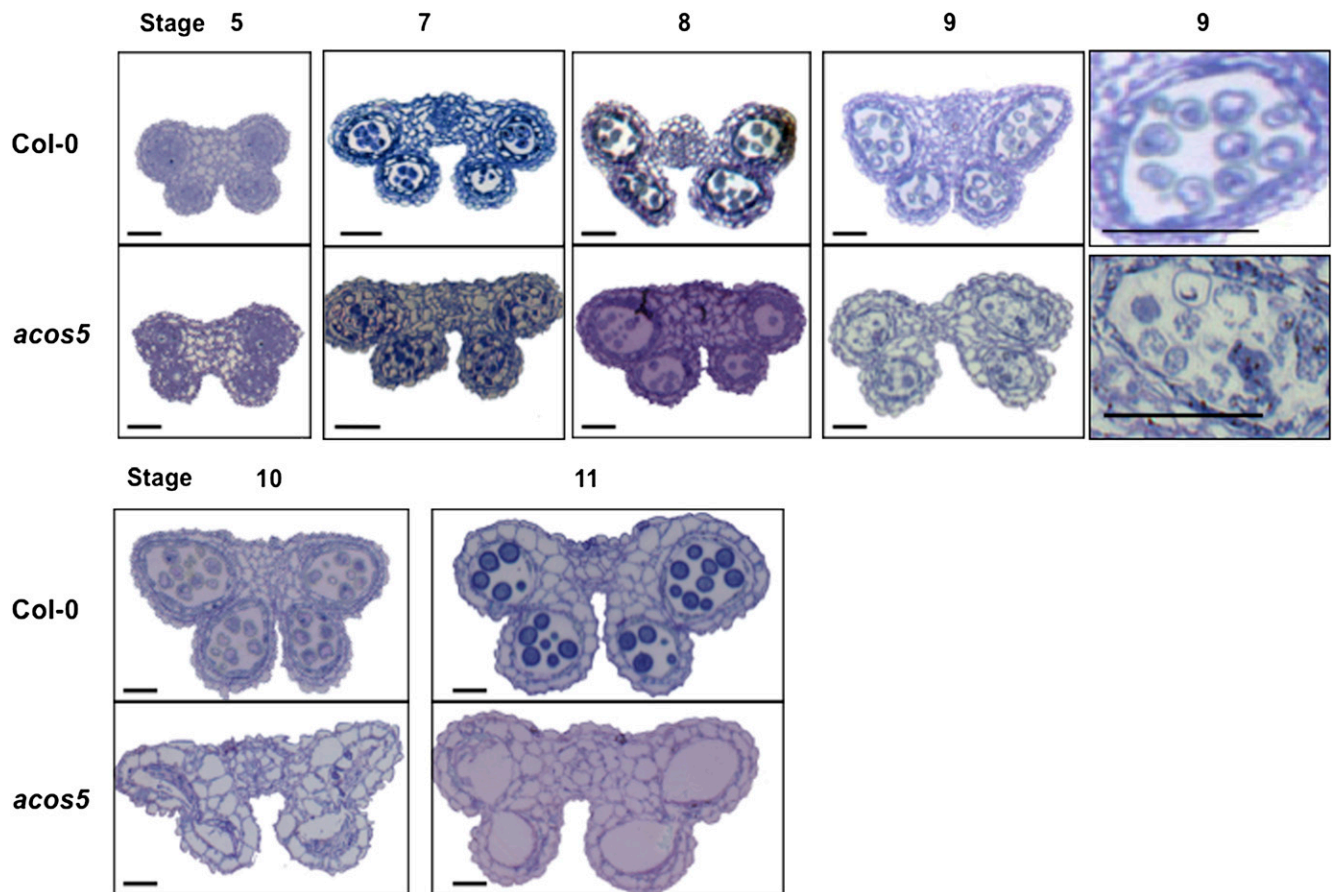


Figure 6. Phenotypic Characterization of Anther and Microspore Development in Wild-Type (Col-0) and *acos5* Flowers.

Anther cross sections (1 μm) were taken from developing flowers of the indicated genotypes. Numbers indicate anther developmental stages according to Sanders et al. (1999). Anther development in *acos5* plants appeared normal until stage 8 (i.e., release of free microspores). At stage 9, initial degradation of microspores was observed, but the tapetal cell layer appeared normal relative to the wild type. By stage 10, microspore degradation was complete in *acos5* plants, whereas maturing pollen grains were observed in wild-type plants. Mature mutant anthers appeared normal but were devoid of pollen grains. Bars = 40 μm .

[See online article for color version of this figure.]

tapetum. By stage 8, during which microspores were released from tetrads, hybridization to tapetal cells weakened and disappeared by stage 11. Similarly, GUS reporter activity was restricted to the tapetum in transgenic lines harboring the 1030-bp *ProACOS5::GUS* fusion (Figure 8B). Collectively, these results demonstrate that *ACOS5* expression is highly specific to tapetal cells and is highest in the stages immediately preceding the appearance of the visible phenotype at stage 8. The results are consistent with an *ACOS5* function in tapetal cells, which are known to be the sites for the biosynthesis of sporopollenin precursors required for exine formation in developing microspores (Goldberg et al., 1993; Sanders et al., 1999; Scott et al., 2004; Ma, 2005).

Biochemical Function of *ACOS5*

We previously described the heterologous expression of *ACOS5* in *Escherichia coli* and its application in a substrate/activity

screen using an ATP depletion assay (Kienow et al., 2008). Among >80 potential substrates tested, *in vitro* activity was observed only against several long-chain fatty acids (i.e., octadecanoic, oleic, linoleic, and linolenic acids), suggesting that *ACOS5* possibly functions as a fatty acyl-CoA synthetase. This activity was confirmed *in vivo* by the capacity of *ACOS5* to complement the deficient acyl-CoA synthetase in the *E. coli fadD* mutant by rescuing growth on oleic acid (C18:1) (Kienow et al., 2008). Further analysis showed that *ACOS5* could also rescue growth on saturated medium-chain fatty acids of chain length C8 to C14, whereas *fadD* growth on shorter-chain fatty acids (C6 and C4) was not supported. To extend these results, we used a more sensitive radioactive assay to directly and unequivocally demonstrate activity of recombinant *ACOS5* against fatty acid substrates *in vitro*. When using ^{14}C -labeled oleic acid as a substrate (20 μM), the affinity-purified recombinant *ACOS5* protein displayed specific activities of CoA-ester formation ranging from 36 to 50 pkat/mg protein. Although this activity is

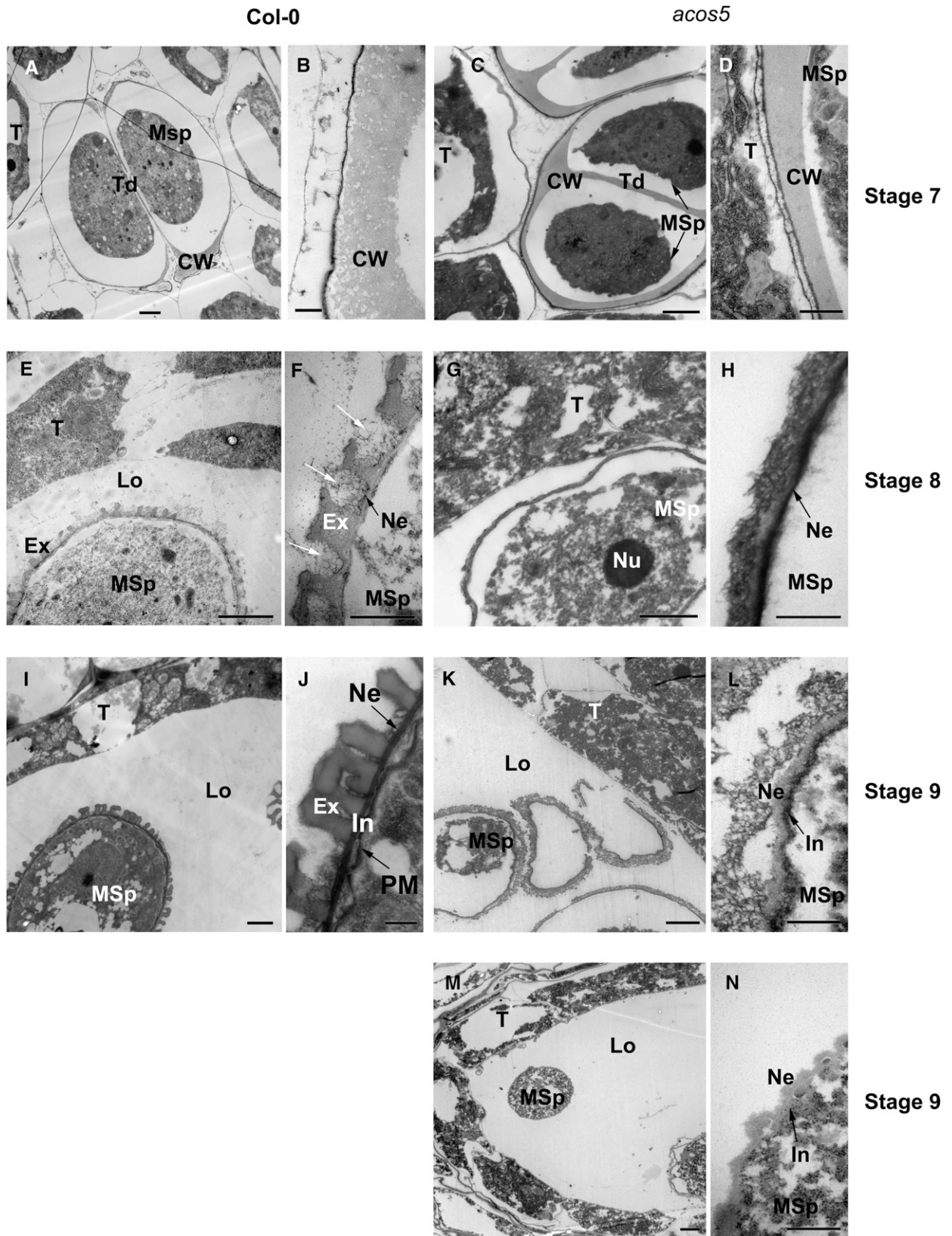


Figure 7. Transmission Electron Micrographs of Wild-Type (*Col-0*) and *acos5* Mutant Anthers, Pollen Grains, and Pollen Walls.

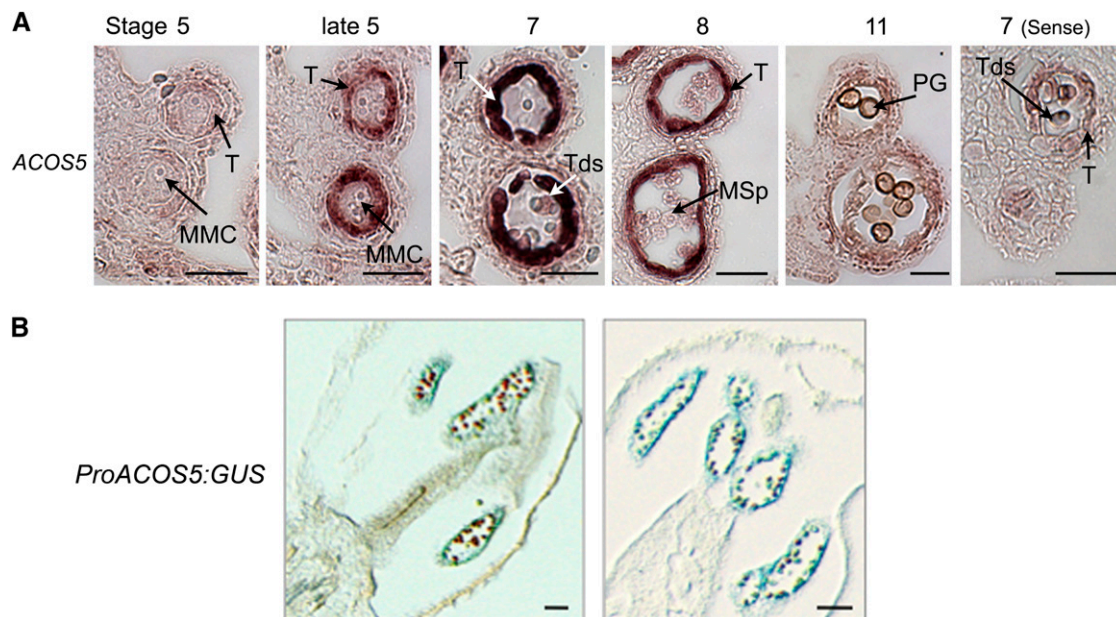


Figure 8. Tapetum-Specific Expression of *ACOS5*.

(A) *ACOS5* mRNA was localized by in situ hybridization to sections taken from developing anther locules of wild-type (Col-0) flowers using a gene-specific antisense probe and a control sense probe. Stages of anther development are according to Sanders et al. (1999). Dark precipitates indicate hybridization of the probe. From left to right: early stage 5 locules with microspore mother cells (MMCs) and a distinct tapetum (T); late stage 5 locules show a hybridization signal in the tapetum; by stage 7, indicated by tetrads (Tds) within the locule, maximal hybridization is detected in the tapetum; the signal in the tapetum weakens by stage 8 and disappears by stage 11; and hybridization with the sense control probe produces no signal. MSP, microspores; PG, pollen grain. Bars = 70 μm.

(B) Tapetum-specific expression of an *ACOS5* promoter-*GUS* fusion. *Arabidopsis* lines homozygous for a single insertion of the reporter gene, comprising a 1030-bp promoter of the *ACOS5* gene and the *GUS* reporter, were generated and. Reporter activity was revealed by X-gluc staining of longitudinal sections of developing anthers. Bars = 80 μm.

low, it is comparable to that of other plant fatty acyl-CoA synthetases expressed in *E. coli* (Fulda et al., 1997; Schnurr et al., 2002, 2004; Shockley et al., 2003). Furthermore, activity was dependent on oleic acid, CoASH, ATP, and native enzyme. The identity of the oleic acid CoA-ester product was verified by mass spectrometry (see Supplemental Table 2 online). The enzyme showed Michaelis-Menten kinetics toward all of substrates, and the derived kinetic parameters are listed in Table 2. The K_m values in the low micromolar range for *ACOS5* substrates have also been reported for other acyl-CoA synthetases (Pongdontri and Hills, 2001; Schnurr et al., 2004; Oba et al., 2005).

To test for the in vitro preference of *ACOS5* for different fatty acid substrates, we applied a competition assay, which determined the conversion of oleic acid (20 μM) to the corresponding

CoA ester in the presence of other potential substrates that acted as competitors. As predicted, addition of unlabeled oleic acid at concentrations of either 50 or 100 μM to the standard reaction mixes decreased the apparent rate of formation of the labeled reaction product to 27 and 15%, respectively (Figure 9A). Among the saturated fatty acids, *ACOS5* showed clear preference for those of medium-chain length (C10 to C14), which competed nearly as well as oleic acid, whereas fatty acids of longer or shorter chain length competed less efficiently (Figures 9A and 9B). When hydroxy fatty acids differing in chain length and substitution pattern were compared, large differences in competition activity were observed. Among the hydroxy-octanoic acids, 8-hydroxy octanoic acid (8OH-C8) competed better than oleic acid, whereas 2OH-C8 and 3OH-C8 were as inactive as

Figure 7. (continued).

(A), (B), (E), (F), (I), and (J) Microspore and pollen wall development in Col-0 wild-type plants.

(C), (D), (G), (H), and (K) to (N) Microspore and pollen wall development in *acos5* mutants.

(A) to (D) Stage 7 anthers.

(E) to (H) Stage 8 anthers.

(I) to (N) Stage 9 anthers.

White arrows in **(F)** indicate residual primexine in developing baculae of the exine. CW, callose wall; Ex, exine; In, intine; Lo, locule; Msp, microspore; Ne, nexine; Nu, nucleus; PM, plasma membrane; T, tapetal cell; Td, tetrad. Bars = 2 μm in **(A), (C), (E), (G), (I), (K), and (M)** and 500 nm in **(B), (D), (F), (H), (J), (L), and (N)**.

Table 2. Kinetic Properties of ACOS5

Substrate	K_m (μM)	V_{max} (pkat mg^{-1})	k_{cat} ($\text{s}^{-1} 10^{-3}$)	k_{cat}/K_m ($\text{s}^{-1} \text{M}^{-1}$)
Oleic acid	3.26 ± 1.30	49.2 ± 9.3	2.91 ± 0.55	892 ± 169
Coenzyme A	1.46 ± 0.29	43.5 ± 6.7	2.57 ± 0.39	1762 ± 270
ATP	35.45 ± 6.18	51.0 ± 13.5	3.02 ± 0.80	85 ± 23

Enzyme activity was determined by a radiochemical assay with affinity-purified protein and various concentrations of the substrates listed. All values are the mean \pm SD of at least three independent determinations.

unsubstituted octanoic acid or 5-dodecanolide, which served as a negative control (Figure 9C). Thus, the position of the hydroxyl group is critical for activity. Among the long-chain hydroxy fatty acids tested, 12OH-C18 and 16OH-C16 were the most efficient competitors, the latter exceeding the apparent effectiveness of oleic acid, whereas medium-chain hydroxy fatty acids (10OH-C10 and 12OH-C12) were again less active (Figure 9D). Intriguingly, the oxylipin OPC-8 impaired oleic acid conversion quite efficiently, whereas none of the hydroxycinnamic acids were effective above control values, with the possible exception of caffeic acid (Figure 9E). We confirmed the ability of ACOS5 to generate CoA esters of the hydroxylated fatty acids 8OH-C8 and 16OH-C16 by mass spectrometric analysis of CoA-esters formed in vitro by incubation of ACOS5 with the corresponding acids (see Supplemental Figure 2 online). From these results we conclude that ACOS5 is a medium- to long-chain fatty acyl-CoA synthetase with a preference for substituted fatty acids carrying a hydroxy group at position C8 to C16, whereas activity as a 4CL can be dismissed.

DISCUSSION

In this study, we used reverse genetics to define the functions of a novel gene essential for male fertility and postmeiotic pollen development in *Arabidopsis* and identified putative orthologs in other species, including *Physcomitrella*. ACOS5 encodes an acyl-CoA synthetase with in vitro activity toward medium- to long-chain fatty acids, their hydroxylated derivatives, and other fatty acyl-containing substrates, and it appears to be required for sporopollenin biosynthesis. In the *acos5* loss-of-function mutant, pollen development is arrested after release from tetrads and free microspores are devoid of exine (Figures 6 and 7). A unique feature of the mutant is the complete absence of pollen grains at anther maturity and consequent complete male sterility. While a number of other *Arabidopsis* male sterile mutants with strongly impaired exine and pollen wall development have been described (Aarts et al., 1997; Morant et al., 2007; Persson et al., 2007), such mutants typically retain variable amounts of (abnormal) pollen grains at anther maturity and corresponding low levels of fertility and seed development. By contrast, the *acos5* homozygote line never produced even partially fertile siliques, necessitating maintenance of the mutant lines as heterozygotes. The exceptionally strong male sterile phenotype and lack of exine formation suggests that ACOS5 plays a crucial role in exine formation and sporopollenin biosynthesis.

Function of ACOS5 in Tapetal Cells

The tapetum is an endothelial cell layer highly specialized for the biosynthesis and secretion of maternally derived pollen wall components, such as sporopollenin. The aliphatic and phenolic monomers of sporopollenin are coupled by ether and ester linkages, which contribute to exine structure and function (Scott et al., 2004; Blackmore et al., 2007). The tapetum contribution to exine synthesis and sporopollenin deposition starts while the microspores are still attached in tetrads and continues through the vacuolated stages until the first pollen mitosis is almost completed (Blackmore et al., 2007). The spatio-temporal patterns of ACOS5 gene expression, revealed by in situ hybridization and promoter-reporter fusion expression (Figure 8), are consistent with transient, tapetum-localized functions (occurring maximally at around stage 7 of anther development) at the time of tetrad formation and microspore release, when biosynthesis and secretion of sporopollenin precursors is required. Furthermore, the phenotype associated with loss of ACOS5 function in the *acos1* mutant first appears at stage 8 (Figures 6 and 7), consistent with defects in deposition of a critical secreted sporopollenin component(s), leading to defective microspores. These microspores, when released from tetrads in stage 8 anthers, fail to develop normal exine and are aborted in development by stage 9. Taken together, these data support the hypothesis that the enzyme encoded by ACOS5 is required for production of sporopollenin constituents in the early steps of exine formation.

Despite the wealth of information on postmeiotic anther and pollen development, only a small number of genes encoding enzymes required for sporopollenin biosynthesis have been identified by genetic approaches. The *MS2* gene, defective in the *ms2* mutant, encodes a protein with similarity to a number of fatty acyl reductases, including those with activity against fatty acids and polyketides (Aarts et al., 1997), while the *CYP703A2* gene (defective in *dex2* mutants) encodes an in-chain fatty acid hydroxylase with an in vitro preference for lauric acid (Morant et al., 2007). Both *CYP703A* and *MS2* are tightly coexpressed with ACOS5 (see Supplemental Table 3 online; Morant et al., 2007), and the similarities between the phenotypes of loss-of-function *acos5*, *ms2*, and *dex2* mutants, coupled with the deduced biochemical functions of the corresponding proteins, suggest that they could function in a common biochemical pathway required for sporopollenin monomer biosynthesis. A unique aspect of the *acos5* phenotype, however, is its complete male sterility relative to the low levels of fertility of *ms2* and *dex2* mutants, despite apparent similar defects in sporopollenin deposition and exine formation in all three mutants. One possible explanation for this phenotypic difference is that the ACOS5 protein could act more centrally in a sporopollenin biosynthetic pathway than MS2 and CYP703A2, such that the *acos5* mutant is completely devoid of sporopollenin, while *ms2* and *dex2* mutants retain low, undetected levels of a modified polymer allowing some pollen function to be retained. Thus, in contrast with the interpretation of the results obtained by Morant et al. (2007), our data suggest that sporopollenin deposition during exine formation may be absolutely required for pollen development and seed production in *Arabidopsis* and that a complete block in the sporopollenin biosynthetic pathway in a mutant such as *acos5*

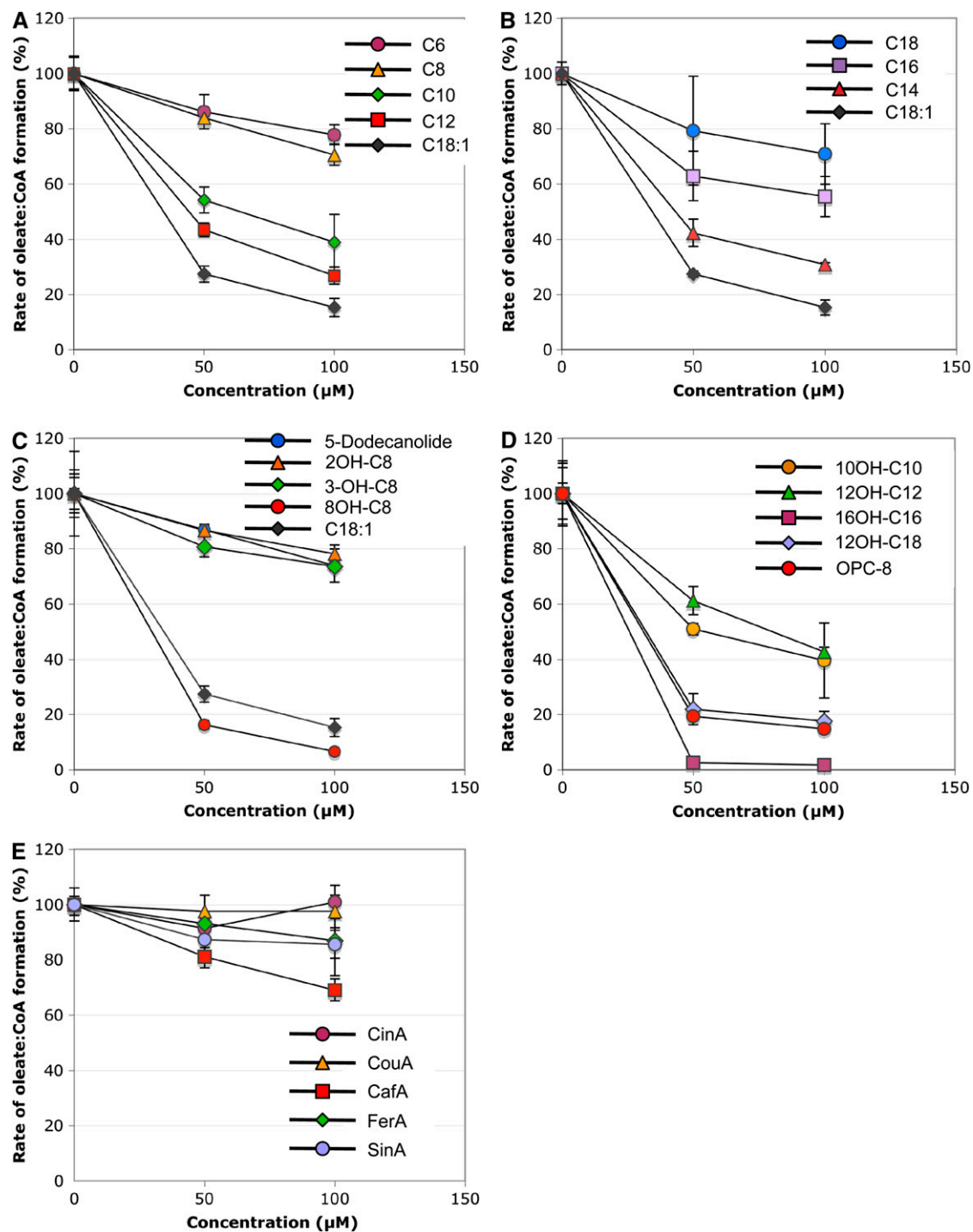


Figure 9. Competition Assays to Assess Substrate Preference of the ACOS5 Acyl-CoA Synthetase.

(A) Short- to medium-chain fatty acids.

(B) Medium- to long-chain fatty acids.

(C) Hydroxylated C8 fatty acids.

(D) Hydroxylated medium- to long-chain fatty acids.

(E) Hydroxycinnamic acids.

Activity of ACOS5 was determined under standard conditions with radiolabeled oleic acid (20 μM) in the absence or presence of the unlabeled competing substrates (each added at 50 or 100 μM). Unlabeled oleic acid (C18:1) was used as positive control, while 5-dodecanolide served as a

leads to complete loss of pollen function and viability prior to anther dehiscence.

An alternative hypothesis for the function of ACOS5 is participation in a vital tapetum-specific metabolic pathway not directly involved in exine formation and sporopollenin biosynthesis, but instead required for basic tapetal cell development and function. In this case, loss of ACOS5 function would indirectly lead to aberrant pollen wall formation and abortion of pollen grain development due to a basic biochemical or developmental defect in tapetal cells. However, as shown in Figure 7, we did not observe any obvious aberrations in the appearance of the tapetum in the *acos5* mutant, suggesting that tapetal function itself is not strongly affected in the mutants (Figure 7). In addition, our *in situ* hybridization results showed that ACOS5 expression in the tapetum is transient and restricted largely to stages 7 and 8 of anther development, returning to background levels well before initiation of normal tapetal degeneration at stages 10 and later. This expression pattern, coupled with the apparently normal tapetal cell morphology in the *acos5* mutant through state 9, is consistent with a role for ACOS5 in a pathway specific for the biosynthesis of sporopollenin monomeric constituents required for exine formation, rather than in the functioning of the tapetum itself.

A number of genes encoding enzymes involved in fatty acid metabolism have been shown to be expressed in tapetal cells over the course of anther development, which like ACOS5 could contribute to sporopollenin biosynthesis. For example, in addition to the *MS2* and *CYP703A2* genes discussed above, the wheat (*Triticum aestivum*) *TAA1* gene encodes a putative tapetum-localized fatty acyl reductase that is capable of generating medium- to long-chain fatty alcohols in tobacco and *E. coli* (Wang et al., 2002), suggesting that it could work downstream of a fatty acyl-CoA synthetase, such as ACOS5. Wang and Li (2008) recently identified a cotton (*Gossypium hirsutum*) acyl-CoA synthetase, ACS1, that is required for male fertility and pollen development in the early stages of microsporogenesis in cotton. However, while expressed in cotton tapetal cells, ACS1 has a broader expression domain than ACOS5 that includes microspores themselves. Furthermore, loss of ACS1 function affects microspore development at a much earlier stage than the *acos5* mutant, with defects in microspore development observed at the pollen mother cell and tetrad stages, resulting in release of aberrant unicellular microspores (Wang and Li, 2008). Finally, we regenerated the protein alignment shown in Supplemental Figure 3A online to include Gh ACS1 and Gh ACS2 (see Supplemental Figure 3B online). A phylogenetic reconstruction of these aligned sequences (see Supplemental Figure 4 and Supplemental Data Set 1 online) indicates that these two cotton acyl-CoA synthe-

tases are not closely related to the clade A ACOS gene family, but instead are most closely related to *Arabidopsis* LACS4, LACS5, and other LACS proteins, with which they share a characteristic LACS linker region absent in 4CL and ACOS proteins (see Supplemental Figure 4B online). This suggests that, in contrast with ACOS5, these cotton enzymes are involved in long-chain fatty acid metabolism required for the early stages of microspore development and unlike ACOS5 may not be directly involved in sporopollenin biosynthesis.

ACOS5 Is an Ancient Acyl-CoA Synthetase Conserved in Land Plants with *In Vitro* Preference for Hydroxylated Medium- to Long-Chain Fatty Acyl Substrates

Arabidopsis contains a large set of adenylate-forming acyl-activating enzymes of diverse functions (Shockey et al., 2003), including four 4CLs active toward hydroxycinnamic acids (Ehltling et al., 1999; Hamberger and Hahlbrock, 2004), nine LACS active toward long-chain fatty acids (Shockey et al., 2002), and *O*-succinylbenzoyl-CoA ligase (Kim et al., 2008). Within the 4CL-like clade of *Arabidopsis* ACOS enzymes (de Azevedo Souza et al., 2008), the peroxisomally localized OPC-8:CoA ligase (OPCL1) is involved in chain shortening reactions in jasmonic acid biosynthesis (Koo et al., 2006; Kienow et al., 2008). Previous work showed that the ACOS5 gene encodes a likely nonperoxisomal acyl-CoA synthetase, closely related to true 4CLs but of unknown biochemical or developmental function (Shockey et al., 2003; de Azevedo Souza et al., 2008). As illustrated in Figure 1, similar enzymes are evolutionarily conserved in angiosperms as well as in *Physcomitrella*, suggesting an ancient and conserved function for this class of genes, which is preferentially expressed in tapetal cells in both *Arabidopsis* (Figure 8) and tobacco (Varbanova et al., 2003) and preferentially in male flowers in poplar (de Azevedo Souza et al., 2008).

Initial analysis of the recombinant ACOS5 protein suggested a lack of activity against hydroxycinnamic acids, substrates typically used by 4CLs (Costa et al., 2005; Kienow et al., 2008), while work reported here (Table 2) demonstrated *in vitro* activity against oleic acid (C18:1) with kinetic constants comparable to those of other fatty acyl-CoA synthetases. Hydroxycinnamic acids failed to compete with oleic acid as ACOS5 substrates (Figure 9), verifying that ACOS5 is not a 4CL. These data suggest that the *in vivo* substrate of ACOS5 is a fatty acid, consistent with a role for ACOS5 in the biosynthesis of an aliphatic sporopollenin monomeric constituent. Moreover, competition assays showed an *in vitro* preference of ACOS5 for medium-chain fatty acids, including hydroxy fatty acids that appear to be important sporopollenin constituents, since they provide the second functional

Figure 9. (continued).

negative control. Other competing substrates were as follows: hexanoic acid (C6), octanoic acid (C8), decanoic acid (C10), dodecanoic acid (C12), tetradecanoic acid (C14), hexadecanoic acid (C16), octadecanoic acid (C18), oleic acid (C18:1), 2-hydroxy octanoic acid (2OH-C8), 3-hydroxy octanoic acid (3OH-C8), 8-hydroxy octanoic acid (8OH-C8), 10-hydroxy decanoic acid (10OH-C10), 12-hydroxy dodecanoic acid (12OH-C12), 16-hydroxy hexadecanoic acid (16OH-C16), 12-hydroxy octadecanoic acid (12OH-C18), 3-oxo-2(2'-[Z]-pentenyl)cyclopentane-1-octanoic acid (OPC-8), cinnamic acid (CinA), coumaric acid (CouA), caffeic acid (CafA), ferulic acid (FerA), sinapic acid (SinA), and 5-dodecanolide (serving as control). All values are the mean \pm SD of at least three determinations (100% corresponding to an activity of 0.35 nkat/mg protein).

group required for the formation of the extensive ether cross-links in the sporopollenin polymer (Ahlers et al., 2000, 2003; Morant et al., 2007). Based on competition assays, the best ACOS5 substrates among those tested were 16-hydroxy hexadecanoic acid (16OH-C16), 8-hydroxy octanoic acid (8OH-C8), and 12-hydroxy octadecanoic acid (12OH-C18). Interestingly, OPC-8, an intermediate in jasmonic acid biosynthesis containing an 8-carbon fatty acyl tail, was also an effective competitor. This suggests that recombinant ACOS5 can bind to and use a variety of substrates in vitro, provided that the substrate fulfills key structural requirements, such as having the polar group (oxygen) in the fatty acid side chain 7 to 15 carbons distal to the carboxy group, which can dramatically increase substrate usage.

While the in planta substrate of ACOS5 remains to be determined, and the lack of defective mature pollen grains in the *acos5* mutant precluded analysis of mutant pollen wall composition, this repertoire of potential substrates is consistent with the deduced aliphatic constituents that form the bulk of cross-linked sporopollenin monomers from several species (Piffanelli et al., 1998; Dominguez et al., 1999; Ahlers et al., 2000; Bubert et al., 2002). It is also consistent with in vivo activity of ACOS5 as an acyl-CoA synthetase that uses a number of fatty acids ranging from C8 to C18 when expressed in *E. coli* (Kienow et al., 2008). The combined in vitro and in vivo data suggest that ACOS5 plays a key role in the biosynthesis of the aliphatic monomeric con-

stituents of sporopollenin by forming fatty acyl-CoA esters of polymer precursors, potentially including the CoA ester of 7-hydroxy lauric acid, which is proposed to be generated by CYP703A2 (Morant et al., 2007). An analogous role for the *Arabidopsis* LACS2 enzyme in biosynthesis of cutin, an aliphatic polyether polymer related to sporopollenin, has been proposed (Schnurr et al., 2004).

Model for the Role of ACOS5 in Sporopollenin Biosynthesis

The combination of our functional data for ACOS5 and similar data for CYP703A and MS2 (Aarts et al., 1997; Morant et al., 2007), and other enzymes localized to the tapetum, such as TAA1 (Wang et al., 2002), provides further insight into potential pathway(s) for generation of sporopollenin monomeric units. Based on these data, we propose a working model for the biosynthesis of sporopollenin monomers (Figure 10). According to this model, the fatty acyl-CoA ester product of the ACOS5 catalyzed reaction is a central intermediate used to generate sporopollenin monomers in tapetal cells for export to the locule. Consistent with a central role for ACOS5 in one or more biochemical pathways leading to sporopollenin monomer biosynthesis is the strong sterility phenotype of the *acos5* mutant and the highly correlated coexpression of ACOS5 with *Arabidopsis* genes encoding enzymes that could act in the same pathway(s),

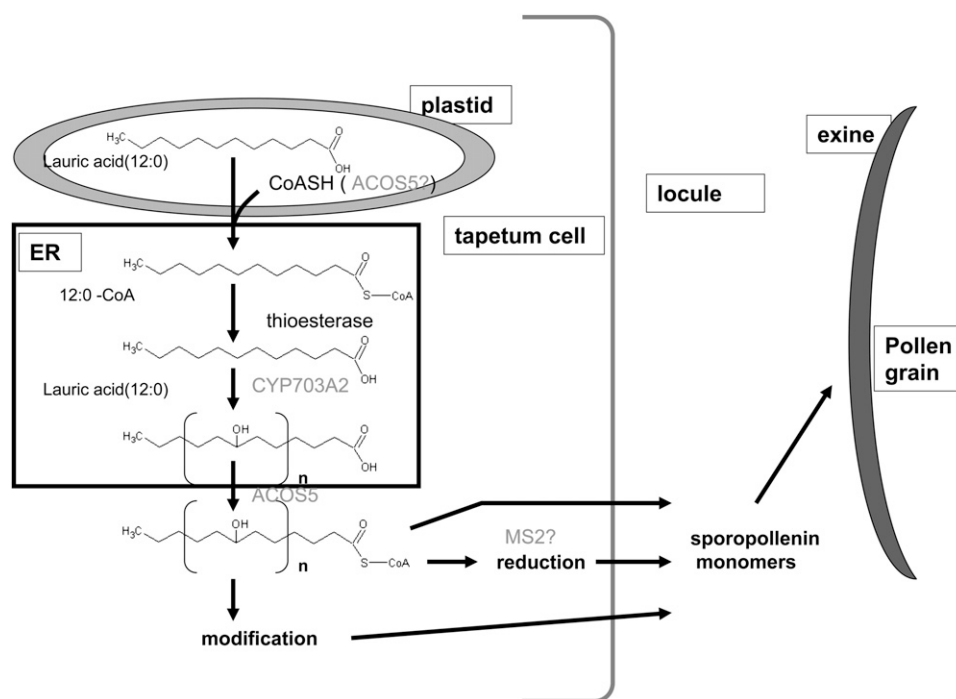


Figure 10. Model for the Role of ACOS5 in Sporopollenin Monomer Biosynthesis in Developing Anthers.

Enzymes encoded by genes with known functions in pollen development and sporopollenin biosynthesis are indicated in grey. The potential cellular and subcellular localization of enzymes in the developing anther is shown. According to this model, the fatty acyl-CoA ester product of the ACOS5 reaction (for example, 7-hydroxylauryl-CoA formed by the action of CYP703A2) could be a central intermediate used to generate sporopollenin monomers by direct transport of the CoA ester to the locule, reduction of the CoA ester to an aldehyde or alcohol followed by transport to the locule, and/or by further modification of the fatty acyl-CoA starter and transport to the locule. CoASH, CoA; ER, endoplasmic reticulum.

including *CYP703A2* and *MS2* (Morant et al., 2007; data not shown).

As shown in Figure 10, one function of ACOS5 could be to regenerate the CoA ester of the proposed hydroxylated fatty acid generated by *CYP703A2* (7-hydroxylauryl-CoA). Such CoA esters are likely required for fatty acid export across the plasma membrane (Schnurr et al., 2004); thus, a loss in ACOS5 activity could prevent secretion of such a hydroxy-fatty acyl sporopollenin monomer. While the formal possibility exists that ACOS5 could function as a plastid localized acyl-CoA synthetase required to generate a fatty acyl-CoA ester for export into the cytoplasm, there is no *in silico* evidence for such localization, and an ACOS5:YFP fusion protein localized to the cytoplasm (Figure 2). Alternatively, or in addition, ACOS5 activity could be required to generate a fatty acyl-CoA substrate for reduction (Figure 10). For example, *MS2* or other tapetum-expressed reductases could generate fatty aldehyde or alcohol monomeric constituents of sporopollenin from the ACOS5-derived CoA ester, which could then be exported into the locule for incorporation into the sporopollenin polymer. Finally, the ACOS5-derived fatty acyl CoA ester could also be used as a starter molecule for incorporation into potentially more complex sporopollenin monomeric constituents, analogous to the incorporation of 4CL-derived *p*-coumaryl-CoA into flavonoids. In this way, the function of ACOS5 in tapetal cells could be analogous to that of 4CL, which generates hydroxycinnamyl-CoA esters used in distinct branch pathways.

Both *CYP703A2* and ACOS5 are conserved in land plant lineages, including *Physcomitrella*, but are absent in *Chlamydomonas* (Morant et al., 2007; de Azevedo Souza et al., 2008; Table 1, Figure 1). Thus, acquisition of an ACOS5- and *CYP703A2*-dependent sporopollenin biosynthetic pathway appears to be an adaptation that was shared by the common terrestrial ancestor of bryophytes and vascular plants. The ability to generate sporopollenin was likely a key land plant innovation essential for protection of haploid spores from desiccation, UV irradiation, and other stresses of the terrestrial environment, and its evolution likely predated vascular system development and the ability to produce lignin (Bowman et al., 2007). Thus, it is conceivable that the repertoire of 4CL and 4CL-related enzymes now found in land plants (Figure 1; de Azevedo Souza et al., 2008) arose from an ACOS5-like ancestral enzyme. Further definition of the biochemical pathway involving ACOS5 should not only reveal the nature of sporopollenin monomeric constituents and the sporopollenin polymer but also shed light on the evolution of the diverse polyether and polyester polymers now found in plants.

METHODS

Plant Material and Growth Conditions

Arabidopsis thaliana wild-type (Col-0) and mutant plants were grown in soil (Sunshine mix 5; Sungrow Horticulture) in controlled environment chambers at 20°C under long-day conditions (18 h light).

Identification and Characterization of an ACOS5 Insertion Mutant

An *Arabidopsis* line with a transposon insertion in ACOS5 (N123936; synonymous with SM_3.37225) was obtained from the NASC and ABRC. Homozygous plants were identified by PCR using primers CLL4F and

EcoRI reverse (see Supplemental Table 4 online) for detection of the endogenous gene, and CLL4F and *dspn1* for detection of the transposon insertion. Homozygous plants were identified by PCR using primers 5RP and 5LP in combination with the T-DNA left-border primer LB1 (see Supplemental Table 4 online).

Crosses of wild-type pollen to homozygous *acos5* mutant plants were performed to obtain F2 generation plants. The patterns of ACOS5 transposon insertion allele segregation in the F2 generations were tested by χ^2 statistical analysis of observed phenotypes and genotypes using GraphPad software (<http://graphpad.com/quickcalcs/chisquared1.cfm>), with expected values based on Mendelian segregation, observed values on the F2 population, and two degrees of freedom (genotypes) or one degree of freedom (phenotypes). The two-tailed P value of >0.4 suggested that the deviation of observed values from expected values was not significant.

Complementation of *acos5* Mutants

A 4368-bp ACOS5 genomic fragment was amplified using the Platinum Taq DNA polymerase High Fidelity (Invitrogen) with gene-specific primers (see Supplemental Table 4 online) and cloned into pCR8/GW/TOPO (Invitrogen). After verification by sequencing, the fragment was subcloned into the pGWB1 Gateway binary vector (Nakagawa et al., 2007) and introduced into *Agrobacterium tumefaciens*. Then, *acos5* heterozygous plants were transformed using the floral dip method (Clough and Bent, 1998). T1 seeds were sown in half-strength Murashige and Skoog salts (Sigma-Aldrich), supplemented with 1% sucrose and 0.6% agar medium containing 25 mg/L hygromycin. Individual T1 lines were allowed to self-pollinate, and progeny genotypes were tested with respect to the ACOS5 locus, and the presence of respective transgenes was tested using PCR with the primers given in Supplemental Table 4 online.

Nucleic Acid Methods

Genomic DNA extraction was performed using young leaf tissue ground in a bead beater at 4°C, with the use of the Nucleon PhytoPure Kit (Amersham-Pharmacia), according to the manufacturer's instructions. *Arabidopsis* RNA was isolated from tissues frozen in liquid nitrogen and ground to a fine powder using Trizol reagent (Gibco-BRL) following the manufacturer's instructions.

RT-PCR

RNA quality was assessed by visual inspection of rRNA on a 1.2% formaldehyde-agarose gel and quantified spectrophotometrically, and 2.5 μ g RNA/20 μ L reaction was used to generate first-strand cDNA using Superscript II Reverse Transcriptase (Invitrogen) following the manufacturer's protocol. For RT-PCR analysis of ACOS5 expression in T-DNA insertion lines, gene-specific and intron-spanning primers (see Supplemental Table 4 online) flanking the sites of the insertions were used in PCR reactions to amplify corresponding cDNA sequences under the following PCR conditions: 95°C for 3 min, 30 cycles of (94°C for 30 s, 56°C for 30 s, and 72°C for 1 min), and 72°C for 10 min, using Taq polymerase in a 50- μ L reaction. PCR products were separated on 1% ethidium bromide agarose gels and photographed under a UV transilluminator using AlphaImager 1220. *Actin1* was used as the control.

Transient Expression and Subcellular Localization of ACOS5 in Planta

The cDNA of ACOS5 was PCR amplified using the primer pair attb1fw-62940 and attb2rv-62940 (see Supplemental Table 4 online) and inserted into the expression vector pENSGYFP, resulting in an N-terminal fusion with YFP using the Gateway cloning system (Invitrogen) as previously described (Schneider et al., 2005). The dsRED fluorescent protein with

the C-terminal extension –SRL served as the peroxisomal marker protein (Schneider et al., 2005). Both vectors allow the in planta expression of proteins under the control of the constitutive cauliflower mosaic virus double 35S promoter. For transient in planta expression, detached leaves of 4-week-old *Arabidopsis* (Col-0) plants were bombarded with 1- μ m gold particles coated with vector DNA using the Biolistic PDS-1000/He Particle Delivery System (Bio-Rad Laboratories) and subsequently placed in a growth chamber for 36 h (Schneider et al., 2005). Fluorescence microscopy was performed using a LSM 510 Meta confocal laser microscope (Carl Zeiss). An argon laser was used as the excitation source (514 nm), and light emission was detected in the range of 570 to 634 nm for RFP constructs and 535 to 545 nm for YFP constructs. Images were recorded and processed using LSM 510 3.2 software (Carl Zeiss).

Generation and Analysis of GUS Reporter Lines

GUS reporter lines of gene *ACOS5* were created using Gateway technology (Invitrogen). Promoter sequences of 1620, 1416, and 1030 bp in length were PCR amplified from *Arabidopsis* (Col-0) genomic DNA using primer pairs Pfw1-62940 and Prv2-62940, Pfw3-62940 and Prv1-62940, and Pfw2-62940 and Prv1-62940, respectively (see Supplemental Table 4 online) and cloned into vector pJawohl11 upstream of *uidA* (*GUS*). The resulting plasmids were transferred into *Arabidopsis* (Col-0) plants by *Agrobacterium*-mediated transformation (Clough and Bent, 1998). Transformants were selected on kanamycin-containing medium, and lines homozygous for a single insertion were identified in the T2 generation. These lines were grown in soil and liquid Murashige and Skoog medium and inspected for GUS expression at different developmental stages and after various treatments. For histochemical staining, seedlings or detached organs were placed in the GUS substrate solution (50 mM sodium phosphate buffer, pH 7.0, 0.1% Triton X-100, 3 mM potassium ferricyanide, 3 mM potassium ferrocyanide, and 1 mM 5-bromo-4-chloro-3-indolyl β -D-glucuronide), and after 5 min of vacuum infiltration, samples were incubated overnight at 37°C and subsequently destained by a series of washes in 80% ethanol (Jefferson, 1987).

Expression and Enzymatic Analysis of Recombinant ACOS5

Heterologous expression in *Escherichia coli* strains DH5 α or M15 and purification of recombinant ACOS5 was performed as previously described (Stuible et al., 2000; Schneider et al., 2005). Enzyme purity was inspected by SDS gel electrophoresis, and protein concentrations were determined according to the Bradford method (Bradford, 1976) with BSA as standard.

Enzymatic activity of the recombinant protein was determined by a luciferase-coupled assay, which records the consumption of ATP, as previously described (Schneider et al., 2005). For detailed kinetic analyses, a more sensitive and accurate radioactive assay using [14 C]oleic acid (specific activity 50 to 62 mCi mmol $^{-1}$; GE Healthcare, Amersham Biosciences) was applied as previously described (Shockey et al., 2002). Briefly, the assay mixture (volume of 100 μ L) contained 100 mM Tris-HCl, pH 7.6, 10 mM MgCl $_2$, 5 mM ATP, 2.5 mM DTT, 1 mM CoASH, 20 μ M oleic acid (dissolved in 0.1% Triton X-100), and 2 μ g of affinity purified protein. The assay was initiated by addition of CoASH (CoA) and incubated at room temperature for 10 min. The reaction was stopped by addition of 100 μ L of 10% (v/v) acetic acid in isopropanol and extracted twice with 900 μ L of hexane (saturated with 50% [v/v] isopropanol). Formation of the oleoyl-CoA ester was quantified in the aqueous phase by liquid scintillation counting, and the identity of the product was confirmed by mass spectrometry (see Supplemental Table 2 online). K_m and V_{max} values were obtained by linear regression of v/s against s (Hanes plots) from at least three independent experiments, in which the corresponding substrate concentrations were varied appropriately. For substrate competition assays, different fatty acids and cinnamic acid derivatives were added

to the standard reaction mixture at 50 or 100 μ M, and formation of oleoyl-CoA was quantified as above. Hydroxy fatty acids and CoA were obtained from Sigma-Aldrich and Fluka.

Phylogenetic and Bioinformatic Analyses

The set of *Arabidopsis* 4CL genes (Ehiting et al., 1999) was used in reciprocal BLAST searches to identify *ACOS5* homologs as previously described by de Azevedo Souza et al. (2008). All sequences obtained are given in Table 1 and Supplemental Table 1 online. Protein sequences were aligned using the Genomatix DIALIGN program (<http://www.genomatix.de/cgi-bin/dialign/dialign.pl>) (Morgenstern, 1999), and the multiple protein sequence alignments were manually optimized. Aligned sequences are shown in Supplemental Figure 3 online. Amino acid sequences used to generate these alignments are shown in Supplemental Data Set 1 online. To reconstruct phylogenetic trees, maximum likelihood analyses with 1000 bootstrap replicates were performed using PhyML v2.4.4 (Guindon and Gascuel, 2003) with the JTT model of amino acid substitution.

Phenotypic Analyses

Scanning electron microscopy was performed using a Hitachi S4700 microscope. Wild-type and homozygous mutant inflorescences were fixed overnight in 2% glutaraldehyde, washed and postfixed in 1% osmium tetroxide in 0.05 M PIPES buffer, pH 7.0, and dehydrated using a series of graded ethanol solutions (30 to 100%). Dried samples were gold sputter coated (Nanotech SEMPRep II sputter coater). To obtain cross sections of developing anthers, wild-type and homozygous mutant inflorescences were fixed in FAA (4% paraformaldehyde, 15% acetic acid, and 50% ethanol) overnight and directly dehydrated without postfixation. Samples were then transferred to a propylene oxide solution and slowly infiltrated with Spurr's epoxy resin (Canemco). For bright-field microscopy, 1- μ m sections were cut with glass knives (Leica) on a microtome, mounted on glass slides, heat fixed to the slides, and stained with toluidine blue. Sections were photographed using a light microscope. All microscopy procedures described were performed in the UBC BioImaging Facility (<http://www.emlab.ubc.ca>).

For transmission electron microscopy, *Arabidopsis* wild-type and *acos5* mutant inflorescences were fixed with paraformaldehyde and postfixed in osmium tetroxide. Fixed samples were dehydrated in an ethanol gradient up to 100% and then transferred to a propylene oxide solution and slowly embedded in Spurr's resin and allowed to polymerize for at least 48 h. Thin sections (70 nm) were taken using a diamond knife microtome (Reichert Ultracut E). Sections were placed on 100-mesh copper grids and stained for 30 min with uranyl acetate and for 15 min with lead citrate (Sato's Lead). Sections were visualized using a Hitachi H7600 transmission electron microscope.

In Situ Hybridization

Arabidopsis Col-0 inflorescences were embedded in Paraplast (Sigma-Aldrich), sectioned at 8 μ m thickness, and mounted onto precharged slides. For sense and antisense *ACOS5* probe synthesis, 526-bp DNA template corresponding to the *ACOS5* coding region was PCR amplified from flower cDNA using gene-specific forward and reverse primers (see Supplemental Table 4 online). A T7 polymerase binding site was incorporated into the forward primer for sense probe amplification and in the reverse primer for antisense probe amplification. Digoxigenin-labeled probes were transcribed off the template using T7 polymerase (Roche). Probes were shortened to 200-bp fragments by limited carbonate hydrolysis, quantified, and hybridized to slides. Tissue fixation, embedding, hybridization, and signal detection are described by Hooker et al. (2002).

Accession Numbers

Sequence data from this article can be found in the Arabidopsis Genome Initiative or GenBank/EMBL databases under the following accession numbers: *Arabidopsis ACOS5*, At1g62940; *Arabidopsis Actin1*, At2g37620. Sequence data for all other genes described in this article can be found in the relevant databases using the accession numbers or gene models given in Supplemental Table 1 online.

Supplemental Data

The following materials are available in the online version of this article.

Supplemental Figure 1. Scanning Electron Micrographs of Wild-Type (Col-0) and *acos5* Mutant Anthers.

Supplemental Figure 2. Mass Spectrometric Analysis of CoA-Esters Formed in Vitro by ACOS5.

Supplemental Figure 3. Alignment of Amino Acid Sequences Used to Generate the Phylogenetic Tree Shown in Figure 1 and Supplemental Figure 4A Online.

Supplemental Figure 4. Relationship of ACOS5 and Clade A Acyl-CoA Synthetase Proteins to Cotton ACS1 and ACS2 Proteins.

Supplemental Table 1. Genes Used for Phylogenetic Reconstruction Shown in Figure 1.

Supplemental Table 2. Molecular Masses of CoA-Ester Products Formed in Vitro from Different Fatty Acids by ACOS5.

Supplemental Table 3. Coexpression of *CYP703A2* and *MS2* with ACOS5.

Supplemental Table 4. Primer Sequences Used for PCR and RNA Probe Generation.

Supplemental Data Set 1. Sequences Used to Generate the Phylogeny Presented in Figure 1 and Supplemental Figure 4A Online.

ACKNOWLEDGMENTS

We thank Bjoern Hamberger and Michael Friedmann for advice and support. We also acknowledge the expert mass spectrometry analyses performed by Thomas Colby. This work was supported by a Discovery Grant from the Natural Sciences and Engineering Research Council of Canada (NSERC) to C.J.D., by an NSERC Discovery Grant to G.W.H., and by the Deutsche Forschungsgemeinschaft (Ko1192/6-3) and the Max Planck Society to E.K.

Received August 8, 2008; revised December 4, 2008; accepted January 27, 2009; published February 13, 2009.

REFERENCES

- Aarts, M.G., Hodge, R., Kalantidis, K., Florack, D., Wilson, Z.A., Mulligan, B.J., Stiekema, W.J., Scott, R., and Pereira, A. (1997). The *Arabidopsis* MALE STERILITY 2 protein shares similarity with reductases in elongation/condensation complexes. *Plant J.* **12**: 615–623.
- Ahlers, F., Bubert, H., Steuernagel, S., and Wiermann, R. (2000). The nature of oxygen in sporopollenin from the pollen of *Typha angustifolia* L. *Z. Naturforsch. [C]* **55**: 129–136.
- Ahlers, F., Lambert, J., and Wiermann, R. (2003). Acetylation and silylation of piperidine solubilized sporopollenin from pollen of *Typha angustifolia* L. *Z. Naturforsch. [C]* **58**: 807–811.
- Ahlers, F., Thoma, I., Lambert, J., Kuckuk, R., and Wiermann, R. (1999). ¹H NMR analysis of sporopollenin from *Typha angustifolia*. *Phytochemistry* **50**: 1095–1098.
- Arizumi, T., Hatakeyama, K., Hinata, K., Sato, S., Kato, T., Tabata, S., and Toriyama, K. (2003). A novel male-sterile mutant of *Arabidopsis thaliana*, faceless pollen-1, produces pollen with a smooth surface and an acetolysis-sensitive exine. *Plant Mol. Biol.* **53**: 107–116.
- Blackmore, S., Wortley, A.H., Skvarla, J.J., and Rowley, J.R. (2007). Pollen wall development in flowering plants. *New Phytol.* **174**: 483–498.
- Blokker, P., Yeloff, D., Boelen, P., Broekman, R.A., and Rozema, J. (2005). Development of a proxy for past surface UV-B irradiation: A thermally assisted hydrolysis and methylation py-GC/MS method for the analysis of pollen and spores. *Anal. Chem.* **77**: 6026–6031.
- Bowman, J.L., Floyd, S.K., and Sakakibara, K. (2007). Green genes - Comparative genomics of the green branch of life. *Cell* **129**: 229–234.
- Bradford, M.M. (1976). A rapid and sensitive method for the quantification of microgram quantities of protein utilizing the principle of protein-dye binding. *Anal. Biochem.* **72**: 248–254.
- Bubert, H., Lambert, J., Steuernagel, S., Ahlers, F., and Wiermann, R. (2002). Continuous decomposition of sporopollenin from pollen of *Typha angustifolia* L. by acidic methanolysis. *Z. Naturforsch. [C]* **57**: 1035–1041.
- Chen, X., Goodwin, S.M., Boroff, V.L., Liu, X., and Jenks, M.A. (2003). Cloning and characterization of the WAX2 gene of *Arabidopsis* involved in cuticle membrane and wax production. *Plant Cell* **15**: 1170–1185.
- Clough, S.J., and Bent, A.F. (1998). Floral dip: A simplified method for *Agrobacterium*-mediated transformation of *Arabidopsis thaliana*. *Plant J.* **16**: 735–743.
- Costa, M., Collins, R., Anterola, A., Cochrane, F., Davin, L., and Lewis, N. (2003). An *in silico* assessment of gene function and organization of the phenylpropanoid pathway metabolic networks in *Arabidopsis thaliana* and limitations thereof. *Phytochemistry* **64**: 1097–1112.
- Costa, M.A., et al. (2005). Characterization *in vitro* and *in vivo* of the putative multigene 4-coumarate:CoA ligase network in *Arabidopsis*: syringyl lignin and sinapate/sinapyl alcohol derivative formation. *Phytochemistry* **66**: 2072–2091.
- Cukovic, D., Ehltling, J., VanZiffle, J.A., and Douglas, C.J. (2001). Structure and evolution of 4-coumarate:coenzyme A ligase (4CL) gene families. *Biol. Chem.* **382**: 645–654.
- Dawson, J., Sozen, E., Vizir, I., Van Waeyenberge, S., Wilson, Z., and Mulligan, B. (1999). Characterization and genetic mapping of a mutation (*ms35*) which prevents anther dehiscence in *Arabidopsis thaliana* by affecting secondary wall thickening in the endothecium. *New Phytol.* **144**: 213–222.
- de Azevedo Souza, C., Barbazuk, B., Ralph, S., Bohlmann, J., Hamberger, B., and Douglas, C. (2008). Genome-wide analysis of a land plant-specific *Acyl:coenzymeA synthetase* (ACS) gene family in *Arabidopsis*, poplar, rice, and *Physcomitrella*. *New Phytol.* **179**: 987–1003.
- Dominguez, E., Mercado, J., Quesada, M., and Heredia, A. (1999). Pollen sporopollenin: Degradation and structural elucidation. *Sex. Plant Reprod.* **12**: 179–193.
- Douglas, C.J., and Ehltling, J. (2005). *Arabidopsis thaliana* full genome longmer microarrays: A powerful gene discovery tool for agriculture and forestry. *Transgenic Res.* **14**: 551–561.
- Edlund, A.F., Swanson, R., and Preuss, D. (2004). Pollen and stigma structure and function: The role of diversity in pollination. *Plant Cell* **16**: S84–S97.
- Ehltling, J., Buttner, D., Wang, Q., Douglas, C.J., Somssich, I.E., and Kombrink, E. (1999). Three 4-coumarate:coenzyme A ligases in

- Arabidopsis thaliana* represent two evolutionarily divergent classes in angiosperms. *Plant J.* **19**: 9–20.
- Ehltig, J., et al.** (2005). Global transcript profiling of primary stems from *Arabidopsis thaliana* identifies candidate genes for missing links in lignin biosynthesis and transcriptional regulators of fiber differentiation. *Plant J.* **42**: 618–640.
- Franke, R., and Schreiber, L.** (2007). Suberin–A biopolyester forming apoplastic plant interfaces. *Curr. Opin. Plant Biol.* **10**: 252–259.
- Fulda, M., Heinz, E., and Wolter, F.P.** (1997). Brassica napus cDNAs encoding fatty acyl-CoA synthetase. *Plant Mol. Biol.* **33**: 911–922.
- Fulda, M., Schnurr, J., Abbadì, A., Heinz, E., and Browse, J.** (2004). Peroxisomal Acyl-CoA synthetase activity is essential for seedling development in *Arabidopsis thaliana*. *Plant Cell* **16**: 394–405.
- Goldberg, R.B., Beals, T.P., and Sanders, P.M.** (1993). Anther development: Basic principles and practical applications. *Plant Cell* **5**: 1217–1229.
- Guilford, W.J., Schneider, D.M., Labovitz, J., and Opella, S.J.** (1988). High resolution solid state ^{13}C NMR spectroscopy of sporopollenins from different plant taxa. *Plant Physiol.* **86**: 134–136.
- Guindon, S., and Gascuel, O.** (2003). A simple, fast, and accurate algorithm to estimate large phylogenies by maximum likelihood. *Syst. Biol.* **52**: 696–704.
- Hamberger, B., Ellis, M., Friedmann, M., de Azevedo Souza, C., Barbazuk, B., and Douglas, C.** (2007). Genome-wide analyses of phenylpropanoid-related genes in *Populus trichocarpa*, *Arabidopsis thaliana*, and *Oryza sativa*: The *Populus* lignin toolbox and conservation and diversification of angiosperm gene families. *Can. J. Bot.* **85**: 1182–1201.
- Hamberger, B., and Hahlbrock, K.** (2004). The 4-coumarate:CoA ligase gene family in *Arabidopsis thaliana* comprises one rare, sinapate-activating and three commonly occurring isoenzymes. *Proc. Natl. Acad. Sci. USA* **101**: 2209–2214.
- Hooker, T.S., Millar, A.A., and Kunst, L.** (2002). Significance of the expression of the CER6 condensing enzyme for cuticular wax production in *Arabidopsis*. *Plant Physiol.* **129**: 1568–1580.
- Hsieh, K., and Huang, A.H.** (2005). Lipid-rich tapetosomes in *Brassica* tapetum are composed of oleosin-coated oil droplets and vesicles, both assembled in and then detached from the endoplasmic reticulum. *Plant J.* **43**: 889–899.
- Hsieh, K., and Huang, A.H.** (2007). Tapetosomes in *Brassica* tapetum accumulate endoplasmic reticulum-derived flavonoids and alkanes for delivery to the pollen surface. *Plant Cell* **19**: 582–596.
- Jefferson, R.A.** (1987). Assaying chimeric genes in plants: The GUS gene fusion system. *Plant Mol. Biol. Rep.* **5**: 387–405.
- Jung, K.H., Han, M.J., Lee, D.Y., Lee, Y.S., Schreiber, L., Franke, R., Faust, A., Yephremov, A., Saedler, H., Kim, Y.W., Hwang, I., and An, G.** (2006). *Wax-deficient anther1* is involved in cuticle and wax production in rice anther walls and is required for pollen development. *Plant Cell* **18**: 3015–3032.
- Kienow, L., Schneider, K., Bartsch, M., Stuible, H.P., Weng, H., Miersch, O., Wasternack, C., and Kombrink, E.** (2008). Jasmonates meet fatty acids: functional analysis of a new acyl-coenzyme A synthetase family from *Arabidopsis thaliana*. *J. Exp. Bot.* **59**: 403–419.
- Kim, H.U., van Oostende, C., Basset, G.J., and Browse, J.** (2008). The AAE14 gene encodes the *Arabidopsis* *o*-succinylbenzoyl-CoA ligase that is essential for phylloquinone synthesis and photosystem-I function. *Plant J.* **54**: 272–283.
- Koo, A.J., Chung, H.S., Kobayashi, Y., and Howe, G.A.** (2006). Identification of a peroxisomal acyl-activating enzyme involved in the biosynthesis of jasmonic acid in *Arabidopsis*. *J. Biol. Chem.* **281**: 33511–33520.
- Kurata, T., Kawabata-Awai, C., Sakuradani, E., Shimizu, S., Okada, K., and Wada, T.** (2003). The YORE-YORE gene regulates multiple aspects of epidermal cell differentiation in *Arabidopsis*. *Plant J.* **36**: 55–66.
- Ma, H.** (2005). Molecular genetic analyses of microsporogenesis and microgametogenesis in flowering plants. *Annu. Rev. Plant Biol.* **56**: 393–434.
- Morant, M., Jorgensen, K., Schaller, H., Pinot, F., Moller, B.L., Werck-Reichhart, D., and Bak, S.** (2007). CYP703 is an ancient cytochrome P450 in land plants catalyzing in-chain hydroxylation of lauric acid to provide building blocks for sporopollenin synthesis in pollen. *Plant Cell* **19**: 1473–1487.
- Morgenstern, B.** (1999). DIALIGN 2: Improvement of the segment-to-segment approach to multiple sequence alignment. *Bioinformatics* **15**: 211–218.
- Nakagawa, T., Kurose, T., Hino, T., Tanaka, K., Kawamukai, M., Niwa, Y., Toyooka, K., Matsuoka, K., Jinbo, T., and Kimura, T.** (2007). Development of series of gateway binary vectors, pGWBs, for realizing efficient construction of fusion genes for plant transformation. *J. Biosci. Bioeng.* **104**: 34–41.
- Oba, Y., Sato, M., Ojika, M., and Inouye, S.** (2005). Enzymatic and genetic characterization of firefly luciferase and *Drosophila* CG6178 as a fatty acyl-CoA synthetase. *Biosci. Biotechnol. Biochem.* **69**: 819–828.
- Paxson-Sowders, D.M., Dodrill, C.H., Owen, H.A., and Makaroff, C.A.** (2001). DEX1, a novel plant protein, is required for exine pattern formation during pollen development in *Arabidopsis*. *Plant Physiol.* **127**: 1739–1749.
- Persson, S., Paredes, A., Carroll, A., Palsdottir, H., Doblin, M., Poindexter, P., Khitrov, N., Auer, M., and Somerville, C.R.** (2007). Genetic evidence for three unique components in primary cell-wall cellulose synthase complexes in *Arabidopsis*. *Proc. Natl. Acad. Sci. USA* **104**: 15566–15571.
- Piffanelli, P., Ross, J.H.E., and Murphy, D.J.** (1998). Biogenesis and function of the lipidic structures of pollen grains. *Sex. Plant Reprod.* **11**: 65–80.
- Pollard, M., Beisson, F., Li, Y., and Ohlrogge, J.B.** (2008). Building lipid barriers: Biosynthesis of cutin and suberin. *Trends Plant Sci.* **13**: 236–246.
- Pongdontri, P., and Hills, M.** (2001). Characterization of a novel plant acyl-coA synthetase that is expressed in lipogenic tissues of *Brassica napus* L. *Plant Mol. Biol.* **47**: 717–726.
- Raes, J., Rohde, A., Christensen, J.H., Van de Peer, Y., and Boerjan, W.** (2003). Genome-wide characterization of the lignification toolbox in *Arabidopsis*. *Plant Physiol.* **133**: 1051–1071.
- Sanders, P., Bui, A., Weterings, K., McIntire, K., Hsu, Y.-C., Lee, P., Truong, M., Beals, T., and Goldberg, R.** (1999). Anther developmental defects in *Arabidopsis thaliana* male-sterile mutants. *Sex. Plant Reprod.* **11**: 297–322.
- Schneider, K., Hovel, K., Witzel, K., Hamberger, B., Schomburg, D., Kombrink, E., and Stuible, H.P.** (2003). The substrate specificity-determining amino acid code of 4-coumarate:CoA ligase. *Proc. Natl. Acad. Sci. USA* **100**: 8601–8606.
- Schneider, K., Kienow, L., Schmelzer, E., Colby, T., Bartsch, M., Miersch, O., Wasternack, C., Kombrink, E., and Stuible, H.-P.** (2005). A new type of peroxisomal acyl-coenzyme A synthetase from *Arabidopsis thaliana* has the catalytic capacity to activate biosynthetic precursors of jasmonic acid. *J. Biol. Chem.* **280**: 13962–13972.
- Schnurr, J., Shockey, J., and Browse, J.** (2004). The acyl-CoA synthetase encoded by *LACS2* is essential for normal cuticle development in *Arabidopsis*. *Plant Cell* **16**: 629–642.
- Schnurr, J.A., Shockey, J.M., de Boer, G.J., and Browse, J.A.** (2002). Fatty acid export from the chloroplast. Molecular characterization of a major plastidial acyl-coenzyme A synthetase from *Arabidopsis*. *Plant Physiol.* **129**: 1700–1709.

- Scott, R.J., Spielman, M., and Dickinson, H.G.** (2004). Stamen structure and function. *Plant Cell* **16** (suppl.): S46–S60.
- Shockey, J.M., Fulda, M.S., and Browse, J.A.** (2002). *Arabidopsis* contains nine long-chain acyl-coenzyme A synthetase genes that participate in fatty acid and glycerolipid metabolism. *Plant Physiol.* **129**: 1710–1722.
- Shockey, J.M., Fulda, M.S., and Browse, J.** (2003). *Arabidopsis* contains a large superfamily of acyl-activating enzymes. Phylogenetic and biochemical analysis reveals a new class of acyl-coenzyme A synthetases. *Plant Physiol.* **132**: 1065–1076.
- Silber, M.V., Meimberg, H., and Ebel, J.** (2008). Identification of a 4-coumarate:CoA ligase gene family in the moss, *Physcomitrella patens*. *Phytochemistry* **69**: 2449–2456.
- Stuible, H.-P., Büttner, D., Ehling, J., Hahlbrock, K., and Kombrink, E.** (2000). Mutational analysis of 4-coumarate:CoA ligase identifies functionally important amino acids and verifies its close relationship to other adenylate-forming enzymes. *FEBS Lett.* **467**: 117–122.
- Taylor, P.E., Glover, J.A., Lavithis, M., Craig, S., Singh, M.B., Knox, R.B., Dennis, E.S., and Chaudhury, A.M.** (1998). Genetic control of male fertility in *Arabidopsis thaliana*: Structural analyses of postmeiotic developmental mutants. *Planta* **205**: 492–505.
- Tuskan, G.A., et al.** (2006). The genome of black cottonwood, *Populus trichocarpa* (Torr. & Gray). *Science* **313**: 1596–1604.
- Varbanova, M.P., Atanassov, A.I., and Atanassov, I.I.** (2003). Anther-specific coumarate CoA ligase-like gene from *Nicotiana sylvestris* expressed during uninucleate microspore development. *Plant Sci.* **164**: 525–530.
- Vizcay-Barrena, G., and Wilson, Z.A.** (2006). Altered tapetal PCD and pollen wall development in the *Arabidopsis ms1* mutant. *J. Exp. Bot.* **57**: 2709–2717.
- Wang, A., Xia, Q., Xie, W., Dumonceaux, T., Zou, J., Datla, R., and Selvaraj, G.** (2002). Male gametophyte development in bread wheat (*Triticum aestivum* L.): Molecular, cellular, and biochemical analyses of a sporophytic contribution to pollen wall ontogeny. *Plant J.* **30**: 613–623.
- Wang, X.L., and Li, X.B.** (2008). The *GhACS1* gene encodes an acyl-CoA synthetase which is essential for normal microsporogenesis in early anther development of cotton. *Plant J.*, in press.
- Yang, C., Xu, Z., Song, J., Conner, K., Vizcay Barrena, G., and Wilson, Z.A.** (2007). *Arabidopsis* MYB26/MALE STERILE35 regulates secondary thickening in the endothecium and is essential for anther dehiscence. *Plant Cell* **19**: 534–548.
- Zhang, W., Sun, Y., Timofejeva, L., Chen, C., Grossniklaus, U., and Ma, H.** (2006). Regulation of *Arabidopsis* tapetum development and function by *DYSFUNCTIONAL TAPETUM1* (*DYT1*) encoding a putative bHLH transcription factor. *Development* **133**: 3085–3095.